Royal Netherlands Institute for Sea Research

Kaiser, J., Schouten, S., Kilian, R., Arz, H.W., Lamy, F. & Sinninhe Damsté, J.S. (2015). Isoprenoid and branched GDGT-based proxies for surface sediments from marine, fjord and lake environments in Chile, *Organic Geochemistry, 89-90*: 117-127

Isoprenoid and branched GDGT-based proxies for surface sediments from marine, fjord and lake environments in Chile

Jérôme Kaiser [a,1,*], Stefan Schouten [a], Rolf Kilian [b], Helge W. Arz [c], Frank Lamy [d], Jaap S. Sinninghe Damsté [a]

[a] *NIOZ Royal Netherlands Institute for Sea Research, Department of Marine Organic Biogeochemistry, P.O. Box 59, 1790 AB Den Burg, Texel, The Netherlands*

[b] *University of Trier, Department of Geology, Behringstrasse, 54296 Trier, Germany*

[c] *Leibniz Institute for Baltic Sea Research (IOW), Seestrasse 15, 18119 Rostock-Warnemünde, Germany*

[d] *Alfred-Wegener-Institute Bremerhaven, Postfach 120161, 27515 Bremerhaven, Germany*

* Corresponding author. Tel.: +4938151973414; fax: +493815197352.

E mail address: jerome.kaiser@io-warnemuende.de (J. Kaiser)

[1] Present address: Leibniz Institute for Baltic Sea Research (IOW), Seestrasse 15, 18119 Rostock-Warnemünde, Germany

ABSTRACT

Proxies based on glycerol dialkyl glycerol tetraether (GDGT) lipids from archaea [isoprenoid GDGTs] and bacteria [branched GDGTs] in 33 surface sediments from marine, fjord and lake systems between 25°S and 50°S in Chile were analyzed. The regional TEX^{H}_{86} calibration obtained from the marine and fjord sediments and mean annual surface temperature ($T = 59.6 \times TEX^{H}_{86} + 33.0$; r^2 0.9; n = 23) is statistically identical to the global ocean calibration based on suspended particulate material in terms of slope, but not in terms of intercept. The regional surface and subsurface TEX^{H}_{86} calibrations were statistically different from the existing global ocean core top calibrations. The TEX_{86} calibration model based on most of the relatively large lakes studied here ($T = 50.7 \times TEX_{86} - 11.8$; r^2 0.9; n = 5) is statistically identical to the global lake calibration. The relatively high TEX_{86} values from smaller lakes suggested an additional source for isoprenoid GDGTs, likely terrestrial or aquatic methanogenic archaea. Application of the soil-calibrated MBT'/CBT (methylation and cyclization of branched (br) GDGTs, respectively) temperature proxy to the marine and fjord sediments resulted in an overestimation of continental mean annual air temperature (MAAT), suggesting in situ production of certain br GDGTs in the water column or surface sediment. For the lakes, MBT'/CBT-based surface air temperature estimates were 3 to 6 °C below MAAT. However, temperature estimates from the lake-specific MBT/CBT global calibration were in good agreement with mean annual surface temperature for all the lakes. The results highlight the need for testing local vs. global calibrations of GDGT-based proxies before their application for palaeoenvironmental reconstruction.

Key words:

GDGT; TEX_{86}; BIT; MBT'; CBT; calibration; marine; fjord; lake; Chile

1. Introduction

Glycerol dialkyl glyceryl tetraethers (GDGTs) are membrane lipids of archaea and bacteria and occur ubiquitously in aquatic environments and soils (reviewed by Schouten et al., 2013). *Thaumarchaeota* (formerly Group 1 Crenarchaeota; Brochier-Armanet et al., 2008; Spang et al., 2010), a specific phylogenetic cluster of the Archaea domain occurring widely in marine and lake systems (e.g. Karner et al., 2001; Keough et al., 2003), biosynthesize isoprenoid (iso) GDGTs (structures in Appendix 1) containing 0-4 cyclopentane moieties and crenarchaeol, which has a cyclohexane moiety in addition to four cyclopentane moieties (Schouten et al., 2000; Sinninghe Damsté et al., 2002; Pitcher et al., 2011a). Another group of GDGTs containing branched (br) instead of isoprenoid alkyl chains (Appendix 1) was initially discovered in peat bogs (Sinninghé Damsté et al., 2000) and subsequently shown to be ubiquitous in soils, coastal marine and lake sediments (e.g. Schouten et al., 2000; Hopmans et al., 2004; Weijers et al., 2006a, 2007a; Sinninghe Damsté et al., 2008; Huguet et al., 2010; Loomis et al., 2011). Acidobacteria thriving in soil are a likely source of brGDGTs (Weijers et al., 2006a, 2009; Sinninghé Damsté et al., 2011, 2014). Although brGDGTs occur mainly in soil and peat, they are probably also produced in situ in the water column and/or the sediments of marine and freshwater (lake and river) environments (e.g. Peterse et al., 2009; Sinninghe Damsté et al., 2009; Tierney and Russell, 2009; Tierney et al., 2010a; Pearson et al., 2011; Zhu et al., 2011; Loomis et al., 2011, 2012, 2014; Zell et al., 2013; Buckles et al., 2014; De Jonge et al., 2014a; Weijers et al., 2014).

Based on the two types of GDGTs, different indices have been developed as palaeoenvironmental proxies. The branched and isoprenoid tetraether (BIT) index uses the abundance of brGDGTs relative to crenarchaeol to estimate the input of soil-derived organic matter (OM) in sediments (e.g. Hopmans et al., 2004; Huguet et al., 2007; Walsh et al., 2008).

The TEX_{86} (tetraether index of GDGTs consisting of 86 carbon atoms) temperature proxy is based on the distribution of aquatic-derived isoGDGTs containing different numbers of cyclopentane moieties (Schouten et al., 2002). Mesocosm incubation studies have shown that the number of cyclopentane moieties in thaumarchaeotal GDGTs increases with growth temperature (Wuchter et al., 2004; Schouten et al., 2007). Global core top marine calibrations suggest that TEX_{86} correlates well with the annual mean temperature of the upper oceanic mixed layer (Kim et al., 2010; Tierney and Tingley, 2014) as well as with the 0-200 m temperature (Kim et al., 2008). Since it appeared that the relative abundance of the crenarchaeol regio-isomer (Appendix 1) is insensitive to temperature change in the polar oceans, a new index was introduced, TEX^{L}_{86}, for application to low temperature (< 15 °C) settings, while TEX^{H}_{86} is more suitable for high temperature settings (> 15 °C; Kim et al., 2010). However, observations suggest that the crenarchaeol regio-isomer (cren'), which is not considered for TEX^{L}_{86}, is essential for SST prediction (Shah et al., 2008; Kim et al., 2010) and in certain polar regions does not perform better than TEX_{86} (Ho et al., 2014). Surveys of lakes indicate that TEX_{86} also correlates with lake surface (Powers et al., 2004, 2010; Blaga et al., 2009) and subsurface temperature (Blaga et al., 2011; Woltering et al., 2012). The relationship between sea/lake surface temperature and TEX_{86} may be masked when a large abundance of soil OM is present in marine or lake sediments, since soils also contain isoGDGTs (albeit in low abundance relative to brGDGTs; Weijers et al., 2006b).

The distribution of brGDGTs is influenced by environmental factors such as pH, temperature and humidity. Weijers et al. (2007a) found that the relative number of cyclopentane moieties, expressed in the cyclization of branched tetraether (CBT) index, is related to soil pH, while the relative number of methyl branches, expressed in the methylation of branched tetraether (MBT) index, is related to both soil pH and mean surface air temperature. Combination of these two indices enables reconstruction of mean air temperature (MAT; Weijers et al., 2007).

Peterse et al. (2012) recently extended the soil dataset and proposed a slightly adjusted index, MBT', using the most commonly occurring brGDGTs in soils. Application of the MBT/CBT index to lake sediments results in large underestimation of mean surface air temperature (e.g. Blaga et al., 2010; Tierney et al., 2010a; Zink et al., 2010), likely due to production of brGDGTs in the water column and/or the sediments (e.g. Sinninghe Damsté et al., 2009; Tierney and Russell, 2009; Buckles et al., 2014). A global calibration of MBT/CBT indices with lake surface temperature was established by Sun et al. (2011), while Tierney et al. (2010a) and Pearson et al. (2011) proposed multiple linear regressions based on the fractional abundances of the most dominant brGDGTs in lake sediments for calibration with mean annual surface temperature. Results based on MBT (MBT') and CBT indices should be carefully considered as a recent study has shown that 6-methyl brGDGTs coelute with 5-methyl brGDGTs (De Jonge et al., 2013), which has led to newly defined indices calibrated against pH and air temperature (De Jonge et al., 2014b). Separation of these isomers requires, however, a special analytical set-up for brGDGT analysis (De Jonge et al, 2013, 2014a,b).

Although GDGT-based proxies are being used increasingly for palaeoclimate reconstruction (e.g. Tierney et al., 2008, 2010b; Lopes dos Santos et al., 2010; Tyler et al., 2010; Caley et al., 2011; Peterse et al., 2011; Kabel et al., 2012; Kim et al., 2012a,b; Ménot and Bard, 2012; Blaga et al., 2013), they still require further validation and calibration for different environmental settings in order to constrain their local and regional applicability and accuracy, as shown by different studies based on soils (e.g. Peterse et al., 2012; Birkholz et al., 2013; De Jonge et al., 2013), marine environments (e.g. Kim et al., 2010; Ho et al., 2011, 2014; Kabel et al., 2012; Tierney and Tingley, 2014) and lake settings (e.g. Blaga et al., 2010, 2011; Huguet et al., 2010; Powers et al., 2010; Tierney et al., 2010a, 2012; Zink et al., 2010; Pearson et al., 2011; Sun et al., 2011; Loomis et al., 2012). While global calibrations indicate that genetic and/or physiological factors exert a relatively small effect on the relationship

between GDGT production and temperature, and are therefore applicable in most environments, regional and local calibrations, which incorporate the influence of e.g. seasonality, production depth and producers, can provide more accurate reconstruction for particular environments (e.g. Sinninghe Damsté et al., 2008; Tierney et al., 2010a; Zink et al., 2010; Kabel et al., 2012; Kim et al., 2015), bearing in mind that these local factors might not have been the same in the past, recent attempts have been undertaken to accommodate this issue by way of the so-called BAYSPAR calibration, which provides local calibrations by considering only data points from a specific spatial grid into account (Tierney and Tingley, 2014). However, data from the southeast Pacific and Chile are still scarce in the global calibrations of GDGT-based temperature proxies (e.g. Kim et al., 2008, 2010; Pearson et al., 2011; Sun et al., 2011; Tierney and Tingley, 2014; Ho et al., 2014). Therefore, in this study, TEX_{86}, TEX^{H}_{86}, as well as the BIT, CBT, MBT and MBT' indices were measured for 33 surface sediments from marine, fjord and lake systems between 25°S and 55°S in Chile. Characterized by strong north-south temperature and rainfall gradients, resulting in drastically contrasting environments, Chile is a suitable region for testing the need for local vs. global calibrations of GDGT-based proxies.

2. Setting

Chile extends between 18°S and 56°S along the southeast Pacific Ocean (Fig. 1). The morphology of the southwestern South American continental margin is characterized by the Andean Cordillera and a coastal range (Weischet, 1970). In southern Chile, the landscape is marked by the presence of the northern and southern Patagonian ice fields, between ca. 46°S and 51°S, and a characteristic fjord system. Often, the fjords are longer than 80 km, with water depth up to 1000 m below sea level (m.b.s.l) and are separated from the open ocean by shallow sills (up to 70 m.b.s.l.). The water column in the fjords is characterized by a two-layer

structure with a strong halocline, resulting from the substantial input of freshwater from rivers (Killian et al., 2007; Sievers, 2008; Silva, 2008).

The Chilean climate is influenced by the presence of a subtropical high pressure cell in the north (around 27°S), associated with virtually no rainfall in northernmost Chile (Atacama Desert) and a low pressure belt around Antarctica (Cerveny, 1998). The resulting southern westerly winds centred around 45-50°S and the presence of the Andes causes extremely high amounts of precipitation exceeding 7 m/yr in the coastal area of southern Chile. From northern to southern Chile annual mean surface air temperature decreases from 14 to 4 °C (Fig. 1) and the mean seasonal amplitude (summer/winter) is ca. 6 °C. Offshore Chile, the westward-flowing Antarctic circumpolar current splits around 45°S into the southward flowing Cape Horn current and the equatorward flowing Peru-Chile Current (PCC; Strub et al., 1998; Chaigneau and Pizarro, 2005; Fig. 1). Driven by east/southeast winds, the PCC is at the origin of an upwelling system along the Chilean coast from ca. 41°S to the equator (Strub et al., 1998). Sea surface temperature (SST) ranges from ca. 20 °C at 18 °S to 7 °C around Cape Horn, with mean seasonal amplitude (summer/winter) ca. 4 °C.

3. Material and methods

The marine, fjord and lake surface sediments (0-1 cm sediment depth) are from an area between 25°S and 55°S (Fig. 1; Table 1). They were recovered during different expeditions: Mascardi lake (December 1993; Ariztegui et al., 1997), ProGlaLakes (January 1994; Chapron et al., 2006), R/V Sonne SO 102 (May-June 1995; Hebbeln et al., 1995), PALATRAS (October 1999; Gilli et al., 2005), R/V Sonne SO 156 (March-May 2001; Hebbeln et al., 2001), Lagos Lanalhue and Lleu Lleu (September 2005), ENDS (March 2006; Waldmann et al., 2010), R/V Gran Campo II cruise in the Chilean Fjords (September 2006), R/V Marion

Dufresne MD 159 PACHIDERME (February 2007) and R/V Gran Campo II expedition to lakes in the Magellanes region (October 2007). The marine sediments (n = 13) were obtained at sites between 25°S and 50°S with a water depth up to 1790 m.b.s.l. The fjord sediments (n = 10) were from sites between 41°S and 54°S at a depth between 40 and 655 m.b.s.l. The lake sediments (n = 10) originate from 6 Chilean lakes and 4 lakes in southern Argentina between 37°S and 55°S at an elevation between 100 and 700 m.a.s.l. (Table 3). The sediments were taken with devices which kept the water-sediment interface undisturbed: multi-corer, short gravity corer and the CASQ gravity corer from the R/V Marion Dufresne.

The total lipid extract (TLE) of the freeze-dried and ground sediment (2-10 g dry weight, dw) was obtained with an accelerated solvent extraction device (DIONEX ASE 200) using dichloromethane (DCM)/MeOH (9:1, v:v) at 100 °C and 1000 psi. After adding 1.0 µg of a C_{46} GDGT as internal standard (Huguet et al., 2006), the extract was separated over an Al_2O_3 column (activated for 2 h at 150 °C) into an apolar, a ketone and a polar fraction using hexane:DCM (9:1 v/v), hexane:DCM (1:1 v/v) and DCM:MeOH (1:1 v/v), respectively. The polar fraction was analyzed for GDGTs as described by Hopmans et al. (2000) and Schouten et al. (2007). An aliquot was dissolved via sonication (5 min) in hexane:propanol (99:1, v/v) and filtered through a 0.45 µm PTFE filter. The sample was analyzed using high performance liquid chromatographyatmospheric pressure chemical ionization mass spectrometry (HPLC-APCI-MS; Agilent 1100 series LC-MS instrument; HP 1100 APCI-MS instrument). Separation was achieved with a Prevail Cyano column (2.1 x 150 mm, 3 µm) maintained at 30 °C. GDGTs were eluted isocratically with 99% hexane and 1% propanol for 5 min, followed by a linear gradient to 1.8% propanol in 45 min. Flow rate was 0.2 ml/min. Conditions for APCI-MS were: nebulizer 60 psi, vaporizer 400 °C, drying gas (N_2) at 6 ml/min and 200°C, capillary voltage -3 kV, corona 5 µA (ca. 3.2 kV). The GDGTs were detected using single ion monitoring (SIM) of the $[M+H]^+$ ions. Quantification was achieved using a relative response

factor value of 1.1 between a C_{46} GDGT standard and an isolated crenarchaeol standard (for details see Huguet et al., 2006). Note that in the present study 5- and 6-methyl brGDGTs were not fully separated with the method used (cf. De Jonge et al., 2013, 2014b).

The GDGT-based indices (Table 2) were calculated following Hopmans et al. (2004) for the BIT index (Eq. 1; Table 2), Schouten et al. (2002) for TEX_{86} (Eq. 2; Table 2), Kim et al. (2010; Eq. 3; Table 2) for TEX^{H}_{86}, Weijers et al. (2007a) for the MBT and CBT indices (Eq. 4 and 5; Table 2) and Peterse et al. (2012) for the MBT' index (Eq. 6; Table 2). As sea surface temperature (SST) data for the Chilean fjords are scarce, unpublished (punctual CTD - conductivity, temperature, depth - data taken during the above expeditions) and few published data from austral winter and spring (Gonzalez et al., 2010, 2011; Palma and Silva, 2004) were used, together with the World Ocean Atlas 2001 database (WOA; Conkright et al., 2002), which has a spatial coverage of 1° x 1° (lat./long.). Depth integrated annual mean temperatures from 0 to 200 m water depth were calculated from WOA following Kim et al. (2008). The WOA temperatures were chosen in the nearest degree in latitude and longitude to each surface sediment position. For surface air temperature, the high resolution (0.1° x 0.1° grid) World Water and Climate Atlas from the International Management Water Institute (IWMI) was used. The atlas is based on an interpolation (which includes elevation as co-predictor) of data from weather stations around the world for 1961-1990 and provides monthly values (New et al., 2002; data available at the IWMI on-line climate summary service portal; http://www.iwmi.cgiar.org/). Mean annual lake surface temperature values were taken from the literature whenever possible (Ariztegui et al., 1997; Parra et al., 2003; Gilli et al., 2005; Pérez et al., 2007; Moy et al., 2011). As both mean annual air and lake surface temperature are similar to each other (Table 3), mean annual air temperature (MAAT) values were used for the lakes when surface water temperature values were not available.

Pearson correlation coefficient analysis and principal component analysis (PCA) were performed with the software PAST (PAleontological STatistics) version 3.04© (Hammer et al., 2001). PCA was performed to identify the dominant factors of the variance in the datasets. Prior to PCA analysis, the data were standardized using mean values and standard deviations to bring all of the variables into proportion with each another. To determine whether the slopes and intercepts of the regression lines were significantly different from each other, *t*-tests were performed using the mean, slope, intercept, standard errors, sum of squared error and sample size for each dataset (Cohen et al., 2003; Wuensch, 2013).

4. Results and discussion

4.1. GDGT concentration and BIT index

The concentration of isoGDGTs (GDGTs 0-3, crenarchaeol and its regio-isomer; Appendices 1 and 2) ranged between 0.2 and 22.4 µg/g dw (mean 6.5 µg/g dw) in the marine sediments and between 4.3 and 15.7 µg/g dw (mean 7.4 µg/g dw) in the fjord sediments (Fig. 2A). The concentration of brGDGTs (summed concentrations of VIII + VII + VI; Appendices 1 and 2) ranged between 0.2 and 0.6 µg/g dw (mean 0.4 µg/g dw) in the fjord sediments and between 0.02 and 0.4 µg/g dw (mean 0.1 µg/g dw) in the marine sediments. The concentration of brGDGTs was highest in the lake sediments, between 0.1 and 2.9 µg/g dw (mean 1.1 µg/g dw), while the mean concentration of isoGDGTs between 0.01 and 1.0 µg/g dw (mean 0.2 µg/g dw) was lower than in the marine and fjord environments.

The BIT index (Eq. 1; Table 2) for the marine sediments ranged between 0.02 and 0.06 (mean 0.03; Fig. 2B), a common value for open marine settings (Schouten et al., 2013 and references therein). For the fjord sediments, values were between 0.04 and 0.08, on average twofold

higher than for the marine sediments. A cross plot of brGDGT concentration and BIT (Fig. 2B) suggests that elevated BIT values in fjord sediments are primarily related to the increase in concentration of brGDGTs, supporting the idea of an increasing contribution of soil OM towards the coastal area. Such a trend was also inferred on the baseis of the interpretation of C/N values from an offshore-inshore transect at ca. 43-47°S. C/N increased from ca. 6 in marine surface sediments (Hebbeln et al., 2000) to 10 and 16 in the outer and inner fjords, respectively (Sepulveda et al., 2011), reflecting an increased input of terrestrial OM, which is characterized by values ≥ 20 (e.g. Meyers, 1994 and references therein). The BIT index seems, therefore, to work well as a proxy for the relative input of soil OM to the marine and fjord environments off Chile. However, in situ production of certain brGDGTs cannot be excluded (Section 4.4.).

The lake sediments had much higher BIT values than the marine and fjord sediments, with values between 0.30 and 0.99 (Fig. 2B), i.e. a common range for lake systems (Schouten et al., 2013 and references therein). In comparison with the other lakes, the sediments from Mascardi, Nahuel Huapi, Cardiel and Fagnano lakes (sediments 9, 10, 22, 33, respectively; Tables 1 and 3) had the lowest BIT values. This may be related to their relatively larger size (Table 3) and a higher in situ thaumarchaeotal productivity (Blaga et al., 2009; Powers et al., 2010; Tierney et al., 2010a, 2012). Indeed, the concentration of crenarchaeol was higher in these lakes than in the other, smaller lakes, which were strongly dominated by brGDGTs (Fig. 2C). There was however no correlation (r^2 0.02; not shown) between BIT values and surface/catchment ratio for the different lakes, as would be expected if brGDGTs are predominantly derived from soils. This may indicate in situ production of certain brGDGTs in the lakes (Section 4.4.).

Using a simple two end member mixing model based on data from the Congo River fan, Weijers et al. (2006b) estimated that BIT index values > 0.3 may bias TEX_{86}-based SST reconstruction by > 2 °C, because isoGDGTs are also present in soils, although in relatively low concentration. Here, TEX_{86}-based SST estimates are unlikely to be biased for the marine and fjord sediments, as all BIT values were < 0.1 (Fig. 2B). The relatively high BIT values for the lake sediments indicate that TEX_{86}-based lake surface temperature may be influenced by soil-derived input of isoGDGTs (cf. Blaga et al., 2009; Powers et al., 2010). However, since in recent years it has become clear that brGDGTs may also be produced in the water column and sediments of lakes (e.g. Sinninghe Damsté et al., 2009; Tierney and Russell, 2009; De Jonge et al., 2014a; Buckles et al., 2014), the BIT index is less reliable in assessing a significant input of soil material to lake systems. Therefore, we also tested the application of the TEX_{86} palaeothermometer to these lakes with BIT values > 0.3.

4.2. TEX^{H}_{86} and temperature in the marine and fjord sediments

Results from water column studies off northern and central-southern Chile have shown that *Thaumarchaeota* are the dominant archaeal group in the Peru-Chile Current system and are predominantly abundant within the upper oxycline (10-100 m depth) of the O_2 minimum zone (OMZ), where NH_4^+ attains maximum concentration (Quiñones et al., 2009; Belmar et al., 2011). Similar results were obtained for the OMZ of the Arabian Sea, with a clear maximum in crenarchaeol concentration at the oxycline (Pitcher et al., 2011b; Schouten et al., 2012). While no data for *Thaumarchaeota* distribution in the water column of the Chilean fjord region were available, the typical two layered structure with an oxycline at ca. 50-75 m and NH_4^+ maximum between 25 and 100 m (Sievers, 2008; Silva, 2008) suggests a potential subsurface habitat of *Thaumarchaeota* in the fjords, as also suspected in a study of Norwegian fjords (Huguet et al., 2007).

In view of the ecological niche of the *Thaumarchaeota*, we tested the values of TEX^{H}_{86} (Eq. 3; Table 2) against observed temperature of both the sea surface (0 m) and subsurface (0-200 m depth-integrated; see Kim et al., 2008) for the marine and fjord sediments, and compared the resulting regional calibrations with the global ones (Fig. 3; Tables 2 and 4). TEX^{H}_{86} values correlated strongly with both SST and subsurface temperature off Chile, but the TEX^{H}_{86} calibrations were statistically different from the global ocean calibrations in terms of slope and intercept (Fig. 3A, B; Table 4). The surface temperature calibration had a statistically similar slope, but a different intercept from the global calibration based on suspended particulate matter (SPM) from < 100 m water depth and in situ temperature (Schouten et al., 2013; Fig. 3C; Tables 2 and 4. Similar results were obtained with the marine sediments only (data not shown), indicating that the different regional relationship between TEX^{H}_{86} and temperature is not caused by the inclusion of fjord sediments. Thaumarchaeota diversity, depth distribution in the water column, as well as seasonality, may explain the difference between the global and our local calibrations. However, the available environmental data are not sufficient to conclude which of these factors cause the observed difference between the calibration off Chile and the global calibration. Our results reveal that the isoGDGT distribution is closely related to surface temperature in both the fjords and the open ocean off Chile, likely because seasonality and depth habitat are similar in both systems. Although *Thaumarchaeota* are probably most abundant at depth (10-100 mwd) off Chile, we recommend using the regional TEX^{H}_{86} surface calibration established here in order to reconstruct annual mean surface palaeotemperature in these environments.

4.3. TEX_{86} in lakes

While there was an apparent relationship between the TEX_{86} values of the sediments of relatively large lakes (water surface > 32 km^2; sediments 6, 7, 9, 10, 22 and 33; Tables 1 and 3) and mean annual lake (air) surface temperatures, the TEX_{86} values for the sediments of relatively small lakes (water surface < 0.1 km^2; sediments 28, 29, 30 and 32; Tables 1 and 3) were much higher than what would be expected from mean annual surface temperature (Fig. 4). This suggests a source of isoGDGTs in addition to water column-dwelling Thaumarchaeota in the relatively small lakes. In order to test this hypothesis, the GDGT-0/crenarchaeol ratio was calculated (Table 3). Since methanogenic archaea synthesize GDGT-0 (Schouten et al., 1998; Koga et al., 1998), but not crenarchaeol, a GDGT-0/crenarchaeol ratio value > 2 indicates that GDGT-0 (and thus also other isoGDGTs such as GDGT-1 and -2) may originate from methanogenic archaea present in lakes (Blaga et al., 2009). While GDGT-0/crenarchaeol values of sediments 28 and 32 were indeed > 2, this was not the case for sediments 29 and 30. Therefore, the input of some isoGDGTs produced by terrestrial and/or aquatic methanogens may explain the elevated TEX^{H}_{86} values observed for certain, but not all, small lakes studied here. For the relatively large lakes, a strong correlation (r^2 0.9) was observed between TEX_{86} values of the sediments (excluding sediment 6, where the GDGT-0/cren ratio was > 2; Table 3) and mean annual lake (air) surface temperatures (Fig. 4). The calibration model [$T = 50.7 \times TEX_{86} - 11.8$; standard error of estimates (SEE) 0.6 °C] is statistically similar to the global lake calibration of Powers et al. (2010) in terms of both slope and intercept (Tables 2 and 4).

4.4. MBT'/CBT indices

The mean BIT values for the marine and fjord sediments (< 0.1) suggest that the soil OM input may be too low for the application of the MBT'/CBT proxy (Eqs. 6 and 7), so the signal may be biased by production of brGDGTs in the marine water column and/or in the sediment

itself (Peterse et al., 2009, 2012; Zhu et al., 2011; Weijers et al., 2014). Indeed, MBT'/CBT MAAT estimates did not correlate (r^2 0; not shown) with observed MAAT values of the adjacent continent (where the brGDGTs were assumed to be derived from Fig. 5A) and were generally ca. 2 to 6 °C higher. The high fractional abundances of brGDGTs with one cyclopentane in the marine and fjord sediments compared with lake sediments as revealed by PCA of the fractional abundance of all 12 analyzed brGDGTs (positive loading of GDGT-VIb and GDGT-VIIb on PC 1, which explained 75% of the variance; Fig. 5B) probably indicates in situ production of brGDGTs (Peterse et al., 2009; Weijers et al., 2014). Indeed, because the porewater of marine sediments is typically alkaline, in situ produced brGDGTs are characterized by a higher degree of cyclization (Peterse et al., 2009). Therefore, a low relative concentration and in situ production of certain brGDGTs prevented the application of the MBT'/CBT proxy to most of the fjord and marine sediments off Chile. However, as brGDGTs with 1-2 cyclopentane moieties mainly are produced in situ in marine sediments (Peterse et al., 2009), the BIT index, which is based on brGDGTs without cyclopentane moieties (Hopmans et al., 2004), is likely not affected by in situ production.

In the lake sediments, a high abundance of soil OM could be expected from the relatively high BIT values (Fig. 2; Table 3). However, in situ production of certain brGDGTs in the water column and/or sediment of lakes has been implied from many studies in a wide variety of regions (Sinninghe Damsté et al., 2009; Tierney and Russell, 2009; Tierney et al., 2010a, 2012; Bechtel et al., 2010; Loomis et al., 2011; Buckles et al., 2014). When the MBT'/CBT soil calibration (Peterse et al., 2012; Eqs. 6 and 7) was applied to the brGDGTs in the lake sediments, a significant correlation (r^2 0.8) existed between estimated and observed mean annual surface (air and lake) temperatures, but the estimated temperature values were ca. 3 to 6 °C below observed values (Fig. 5A). This agrees with previous studies and is likely due to in situ production of brGDGTs in lakes (see above).

Consequently, specific brGDGT calibrations for lake surface water temperature have been developed using lake surface sediments (Tierney et al., 2010a; Pearson et al., 2011; Sun et al., 2011; Loomis et al., 2012). The two global calibrations developed by Sun et al. (2011) and Pearson et al. (2011) were tested for the lakes here (Eqs. 20-21; Table 2). While the Pearson et al. (2011) calibration, based on summer MAT, resulted in estimates ca. 2 to 7 °C above observed mean summer temperatures, the Sun et al. (2011) calibration based on MAAT provided temperature estimates closest to observed mean annual surface temperatures (Fig. 5C). With the latter calibration, estimated and observed temperatures correlated significantly (r^2 0.9) and the slope of the linear regression was close to one (0.8; Fig. 5D). The residuals (< 0.8 °C; not shown) were within the calibration error of ± 4.3 °C (Sun et al., 2011). Therefore, while the absence of water pH data from certain lakes here prevented establishing a MBT/CBT regional calibration, reliable surface temperature estimates could be obtained by applying the global calibration from Sun et al. (2011) for the relatively small lakes, where the TEX_{86} proxy was not applicable (Section 4.3.). For the relatively large lakes, both branched and isoprenoid GDGT-based indices potentially allow reconstructing past lake surface temperature.

5. Conclusions

Different proxies based on isoprenoid and branched GDGTs in 33 surface sediments from open ocean, fjords and lakes in Chile were measured. The results corroborate the application of these organic proxies to the region. For the marine and fjord environments, the BIT index seemed to work well as a proxy for relative inputs of soil OM, although in situ production of some brGDGTs in the water column and/or the sediment cannot be fully excluded. While GDGT distributions were dominated by brGDGTs in lake sediments, brGDGTs were

probably produced predominantly in situ in the water column and/or the sediment. Therefore, the BIT index should not be used as a proxy for soil OM input to these lakes.

The regional calibration of TEX^{H}_{86} with annual mean surface temperature for the fjord and marine sediments was statistically similar to the SPM global calibration in terms of slope, suggesting that GDGT distribution correlates with Thaumarchaeota growth temperature in surface (< 100 m) water of the fjords and open ocean off Chile. The regional TEX_{86} calibration based on most of the relatively large lakes was statistically similar to the global TEX_{86} lake calibration. The production of some isoGDGTs by other (methanogenic) archaea prevented the application of TEX_{86} to relatively small lakes (water surface < 1 km^2).

In situ production of brGDGTs containing a relatively high amount of cyclopentane moieties in the water column and/or in the sediment prevented application of the MBT'/CBT palaeothermometer, using the soil-based calibration from Peterse et al. (2012), to the marine, fjord and lake environments. However, the global lake-specific MBT/CBT calibration of Sun et al. (2011) provided temperature estimates close to observed mean annual surface temperatures for all the lakes here.

Acknowledgments

M. Baas, E. Hopmans and M. Kienhuis are thanked for analytical assistance, as well as F. Peterse for constructive comments. We acknowledge support from the French Polar Institute IPEV, which provided the RV Marion Dufresne and the CASQ coring system used during the IMAGES XV MD159 PACHIDERME cruise (February 2007). D. Ariztegui and D. Hebbeln kindly provided some lake and marine sediments, respectively. J.K. was funded by grant PBSK2-115721/1 from the Swiss National Science Foundation. S.S. was funded by a VICI

grant from the Netherlands Organisation for Scientific Research (NWO). The research received funding from the European Research Council under the European Union's Seventh Framework Programme (FP7/2007-2013)/ERC grant agreement [226600] and by the Netherlands Earth System Science Centre (NESSC), which is financially supported by the Ministry of Education, Culture and Science (OCW). H.W.A. and F.L. received funding from the German Research Foundation (DFG) through projects AR 367/6-1 and LA 1273/7-2. B.D. Naafs and an anonymous reviewer are thanked for suggesting improvements to the original manuscript.

Associate editor – **H.M. Talbot**

Figure, table and appendix captions

Fig. 1. (A) Distribution of mean annual SST (contour lines; data from World Ocean Atlas 2001; Conkright et al., 2002) and air temperature (data from New et al., 2002). Arrows represent the main ocean surface currents in the southeast Pacific region (ACC, Antarctic Circumpolar Current; PCC, Peru-Chile Current; CHC, Cape Horn Current). (B) Detailed map with location of the surface sediments from marine (circles), fjord (triangles) and lake (stars) environments (see Tables 1 and 3).

Fig. 2. (A) Concentrations of branched vs. isoprenoid GDGTs of the marine, fjord and lake sediments. (B) BIT index values vs. amount of brGDGTs (log scale). The dotted line represents the upper limit below which TEX_{86} indices are assumed not to be biased by soil-derived GDGTs (Weijers et al., 2006b; see text for details). (C) Relative abundance of crenarchaeol and brGDGTs in the lake sediments. Numbers refer to sediments listed in Table 1.

Fig. 3. Regional calibration lines for TEX^{H}_{86} and (A) annual mean surface (0 m) and (B) subsurface (integrated depth 0-200 m) temperature in comparison with global calibration curves. Circles and triangles represent marine and fjord sediments off Chile, respectively, and the grey dots the data used in the global calibrations from Kim et al. (2010, 2012a,b). Numbers refer to sediments in Table 1. See Table 2 for the equations of all calibration curves.

Fig. 4. Correlation between TEX_{86} and mean annual surface temperature for relatively large (black stars) and small (grey stars) lakes. Note that sediment 6 was not included in the linear regression based on relatively large lakes (see text for details). The global correlation curve from Powers et al. (2010; Eq. 12; Table 2) is also shown (grey dashed line). Numbers refer to sediments in Table 1.

Fig. 5. (A) Comparison between observed and estimated mean annual surface temperature using the MBT'/CBT soil-based calibration (Peterse et al., 2012; Eq. 14; Table 2) for the marine, fjord and lake sediments. Numbers refer to the sediments in Table 1. (B) PCA of the fractional abundance of brGDGTs in the marine, fjord and lake sediments. Roman numerals refer to structures in Appendix 1 and numbers to the sediments in Table 1. (C) Comparison of observed and estimated surface temperature using the different brGDGT-based indices and lake-specific calibrations from Sun et al. (2011; Eq. 15; Table 2) for mean annual temperature estimates and from Pearson et al. (2011; Eq. 16; Table 2) for mean summer temperature estimates. (D) Linear regression between observed and estimated mean annual surface temperature for the lakes using the global lake calibration from Sun et al. (2011; Eq. 15; Table 2).

Table 1

Sediment label, location, observed surface (0 m) and subsurface (0-200 m) mean annual water temperatures and values for the different GDGT-based indices (n.d., no data.

Table 2

GDGT-based indices and reported global and regional (this study) calibration curves (fr, fractional abundance; SEE, standard error of estimate; roman numerals refer to structures in Appendix 1).

Table 3

General characteristics of sampled lakes (m.a.s.l., m above sea level; n.d., no data; BIT is defined in Table 2).

Table 4

Similarity of slopes and intercepts of different calibration curves considered in this study (see equations 7-13 in Table 2). A *t*-test probability value < 0.05 (in italics) indicates that the slopes/intercepts are significantly different from each other (Cohen et al., 2003; Wuensch, 2013). Tests for the intercepts were not performed when the homogeneity of slope tests were not fulfilled (i.e. no parallel linear relationship between the covariate and the dependant variable) as an invalid analysis of the intercepts may result in inaccurate data interpretation (Hinkle et al., 2003).

Appendix 1. Structures of the isoprenoid and branched GDGT membrane lipids.

Appendix 2. Abundances (ng/g dw) of isoprenoid (GDGT-0, -1, -2, -3, -4, -4') and branched (GDGT-VI, -VIa, -VIb, -VII, -VIIa, -VIIb, -VIII, -VIIIa, -VIIIb) GDGTs in the surface sediments. See Appendix 1 for the structures of the GDGTs.

References

Ariztegui, D., Bianchi, M.M., Masaferro, J., Lafargue, E., Niessen, F., 1997. Interhemispheric synchrony of Late-glacial climatic as recorded in proglacial Lake Mascardi, Argentina. Journal of Quaternary Sciences 12, 333-338.

Bechtel, A., Smittenberg, R.H., Bernasconi, S.M., Schubert, C.J., 2010. Distribution of br and iso tetraether lipids in an oligotrophic and a eutrophic Swiss lake: Insights into sources and GDGT-based proxies. Organic Geochemistry 41, 822-832.

Belmar, L., Molina, V., Ulloa, O., 2011. Abundance and phylogenetic identity of archaeoplankton in the permanent oxygen minimum zone of the eastern tropical South Pacific. Federation of European Microbiological Societies Microbiology Ecology 78, 314-326.

Birkholz, A., Smittenberg, R.H., Hajdas, I., Wacker, L., Bernasconi, S.M., 2014. Isolation and compound specific radiocarbon dating of terrigenous br glycerol dialkyl glycerol tetraethers (brGDGTs). Organic Geochemistry 60, 9-19.

Blaga, C.I., Reichart, G.-J., Heiri, O., Sinninghe Damsté, J.S., 2009. Tetraether membrane lipid distributions in water-column particulate matter and sediments: A study of 47 European lakes along a north-south transect. Journal of Paleolimnology 41, 523-540.

Blaga, C.I., Reichart, G-J., Schouten, S., Lotter, A.F., Werne, J.P., Kosten, S., Mazzeo, N., Lacerot, G., Sinninghe Damsté, J.S., 2010. Br glycerol dialkyl glycerol tetraethers in lake

sediments: Can they be used as temperature and pH proxies?. Organic Geochemistry 41, 1225-1234.

Blaga, C.I., Reichart, G.-J., Vissers, E.W., Lotter, A.F., Anselmetti, F.S., Sinninghe Damsté, J.S., 2011. Seasonal changes in glycerol dialkyl glycerol tetraether concentrations and fluxes in a perialpine lake: Implications for the use of the TEX_{86} and BIT proxies. Geochimica et Cosmochimica Acta 75, 6416-6428.

Blaga, C.I., Reichart, G.-J., Lotter, A.F., Anselmetti, F.S., Sinninghe Damsté, J.S., 2013. A TEX_{86} lake record suggests simultaneous shifts in temperature in Central Europe and Greenland during the last deglaciation. Geophysical Research Letters 40, 948-953.

Brochier-Armanet, C., Boussau, B., Gribaldo, S., Forterre, P., 2008. Mesophilic crenarchaeota: proposal for a third archaeal phylum, the Thaumarchaeota. Nature Reviews Microbiology 6, 245-252.

Buckles, L.K., Weijers, J.W.H., Verschuren, D., Sinninghe Damsté, J.S., 2014. Sources of core and intact br tetraether membrane lipids in the lacustrine environment: Anatomy of Lake Challa and its catchment, equatorial East Africa. Geochimica et Cosmochimica Acta 140, 106-126.

Caley, T., Kim, J.-H., Malaizé, B., Giraudeau, J., Laepple, T., Caillon, N., Charlier, K., Rebaubier, H., Rossignol, L., Castañeda, I.S., Schouten, S., Sinninghe Damsté, J.S., 2011. High-latitude obliquity as a dominant forcing in the Agulhas current system. Climate of the Past 7, 1285-1296.

Chaigneau, A., Pizarro, O., 2005. Mean surface circulation and mesoscale turbulent flow characteristics in the eastern South Pacific from satellite tracked drifters. Journal of Geophysical Research C 110, 1-17.

Chapron, E., Ariztegui, D., Mulsow, S., Villalba, G., Pino, M., Charlet, F., 2006. Impact of 1960 major subduction earthquake in northern Patagonia (Chile-Argentina). Quaternary International 158, 58-71.

Cohen, J., Cohen, P., Stephen, G.W., Leona, S.A., 2003. Applied Multiple Regression/Correlation Analysis for the Behavioral Sciences, third ed. L. Erlbaum Associates, Mahwah, New Jersey.

Conkright, M.E., Locarnini, R.A., Garcia, H.E., O'Brien, T.D., Boyer, T.P., Stephens, C., Antonov, J.I., 2002. World Ocean Atlas 2001: Objective Analyses, Data Statistics. National Oceanographic Data Center, Silver Spring, MD, 17 pp.

De Jonge, C., Hopmans, E.C., Stadnitskaia, A., Rijpstra, A.W.I., Hofland, R., Tegelaar, E., Sinninghe Damsté, J.S., 2013. Identification of novel penta- and hexamethylated br glycerol dialkyl glycerol tetraethers in peat using HPLC–MS^2, GC–MS and GC–SMB-MS. Organic Geochemistry 54, 78-82.

De Jonge, C., Stadnitskaia, A., Hopmans, E.C., Cherkashov, G., Fedotov, A., , Sinninghe Damsté, J.S., 2014a. In situ produced br glycerol dialkyl glycerol tetraethers in suspended particulate matter from the Yenisei River, Eastern Siberia. Geochimica et Cosmochimica Acta 125, 476-491.

De Jonge, C., Hopmans, E.C., Zell, C.I., Kim, J.-H., Schouten, S., Sinninghe Damsté, J.S., 2014. Occurrence and abundance of 6-methyl branched glycerol dialkyl glycerol tetraethers in soils: Implications for palaeoclimate reconstruction. Geochimica et Cosmochimica Acta 141, 97-112.

Gilli, A., Ariztegui, D., Anselmetti, F.S., McKenzie, J.A., Markgraf, V., Hajdas, I., McCulloch, R.D., 2005. Mid-Holocene strengthening of the southern westerlies in South America – Sedimentological evidences from Lago Cardiel, Argentina (49°S). Global and Planetary Change 49, 75-93.

González, H.E., Calderón, M.J., Castro, L., Clement, A., Cuevas, L.A., Daneri, G., Iriarte, J.L., Lizárraga, L., Martínez, R., Menschel, E., Silva, N., Carrasco, C., Valenzuela, C., Vargas, C.A., Molinet C., 2010. Primary production and plankton dynamics in the Reloncaví Fjord and the Interior Sea of Chiloé, Northern Patagonia, Chile. Marine Ecology-Progress Series 402, 13-30.

González, H.E., Castro, L., Daneri, G., Iriarte, J.L., Silva, N., Vargas, C.A., Giesecke, R. Sánchez, N., 2011. Seasonal plankton variability in Chilean Patagonia fjords: Carbon flow through the pelagic food web of Aysen Fjord and plankton dynamics in the Moraleda Channel basin. Continental Shelf Research 31, 225-243.

Hammer, Ø., Harper, D.A.T., Ryan, P.D., 2001. PAST: Paleontological statistics software package for education and data analysis. Palaeontologia Electronica 4, 1-9.

Hebbeln, D. and shipboard scientists, 1995. Cruise Report of R/V Sonne Cruise SO-102, Valparaiso (Chile) - Valparaiso (Chile), May 09 - June 28 1995, Berichte Fachbereich Geowissenschaften, Universität Bremen, Bremen, Germany, 126 pp.

Hebbeln, D., Marchant, M., Freudenthal, T., Wefer, G., 2000. Surface sediment distribution along the Chilean continental slope related to upwelling and productivity. Marine Geology 164, 119-137.

Hebbeln, D. and shipboard scientists, 2001. PUCK: Report and Preliminary Results of R/V Sonne Cruise SO156, Valparaiso (Chile)-Talcahuano (Chile), March 29 – May 14 2001. Berichte Fachbereich Geowissenschaften, Universität Bremen, Bremen, Germany, 195 pp.

Hinkle, D., Wiersman, W., Jurs, S., 2003. Applied Statistics for the Behavioral Sciences. Houghton Mifflin Co., Boston, 756 pp.

Ho, S.L., Yamamoto, M., Mollenhauer, G., Minagawa, M., 2011. Core top TEX_{86} values in the south and equatorial Pacific. Organic Geochemistry 42, 94-99.

Ho, S.L., Mollenhauer, G., Fietz, S., Martínez-García, A., Lamy, F., Rueda, G., Schipper, K., Méheust, M., Rosell-Melé, A., Stein, R., Tiedemann, R., 2014. Appraisal of TEX_{86} and TEX^{L}_{86} thermometries in subpolar and polar regions. Geochimica et Cosmochimica Acta 131, 213-226.

Hopmans, E.C., Schouten, S., Pancost, R.D. , van der Meer, M.T.J., Sinninghe Damsté, J.S., 2000. Analysis of intact tetraether lipids in archaeal cell material and sediments by high

performance liquid chromatography/atmospheric pressure chemical ionization mass spectrometry. Rapid Communications in Mass Spectrometry 14, 585–589.

Hopmans, E.C., Weijers, J.W.H., Schefuss, E., Herfort, L., Sinninghe Damsté, J.S., Schouten, S., 2004. A novel proxy for terrestrial organic matter in sediments based on br and iso tetraether lipids. Earth and Planetary Science Letters 224, 107-116.

Huguet, C., Hopmans, E.C., Febo-Ayala, W., Thompson, D.H., Sinninghe Damsté, J.S., Schouten, S., 2006. An improved method to determine the absolute abundance of glycerol dibiphytanyl glycerol tetraether lipids. Organic Geochemistry 37, 1036-1041.

Huguet, C., Smittenberg, R.H., Boer, W., Sinninghe Damsté, J.S., Schouten, S., 2007. Twentieth century proxy records of temperature and soil organic matter input in the Drammensfjord, southern Norway. Organic Geochemistry 38, 1838-1849.

Huguet, A., Fosse, C., Laggoun-Défarge, F., Toussaint, M-L., Derenne, S., 2010. Occurrence and distribution of glycerol dialkyl glycerol tetraethers in a French peat bog. Organic Geochemistry 41, 559-572.

Kabel, K., Moros, M., Porsche, C., Neumann, T., Adolphi, F., Andersen, T.J., , Siegel, H., Gerth, M., Leipe, T., Jansen, E., Sinninghe Damsté, J.S., 2012. Impact of climate change on the Baltic Sea ecosystem over the past 1,000 years. Nature Climate Change 2, 871–874.

Karner, M.B., Delong, E.F., Karl, D.M., 2001. Archaeal dominance in the mesopelagic zone of the Pacific Ocean. Nature 409, 507-510.

Keough, B.P., Schmidt, T.M., Hicks, R.E., 2003. Archaeal nucleic acids in picoplankton from Great Lakes on three continents. Microbial Ecology 46, 238-248.

Kilian, R., Baeza, O., Steinke, T., Arevalo, M. Rios, C., Schneider, C., 2007. Late Pleistocene to Holocene marine transgression and thermohaline control on sediment transport in the western Magellanes fjord system of Chile (53°S). Quaternary International 161, 90-107.

Kim J.-H., Schouten, S., Hopmans, E.C., Donner, B., Sinninghe Damsté, J.S., 2008. Global sediment core top calibration of the TEX_{86} paleothermometer in the ocean. Geochimica et Cosmochimica Acta 72, 1154-1173.

Kim, J-H., van der Meer, M.J.T., Schouten, S., Helmke, P., Willmott, V., Sangiorgi, F., Koc, N., Hopmans, E.C., Sinninghe Damsté, J.S., 2010. New indices and calibrations derived from the distribution of crenarchaeal iso tetraether lipids: Implications for past sea surface temperature reconstructions. Geochimica et Cosmochimica Acta 74, 4639-4654.

Kim, J.-H., Crosta, X, Willmott, V., Renssen, H., Bonnin, J., Helmke, P., Schouten, S., Sinninghe Damsté, J.S., 2012a. Holocene subsurface temperature variability in the eastern Antarctic continental margin. Geophysical Research Letters 39, L06705.

Kim, J.-H., Romero, O.E., Lohmann, G., Donner, B., Laepple, T., Haam, E., Sinninghe Damsté, J.S., 2012b. Pronounced subsurface cooling of North Atlantic waters off Northwest Africa during Dansgaard–Oeschger interstadials. Earth and Planetary Science Letters, 339–340, 95-102.

Kim, J.-H., Schouten, S., Rodrigo-Gámiz, M., Rampen, S., Marino, G., Huguet, C., Helmke, P., Buscail, R., Hopmans, E.C., Pross, J., Sangiorgi, F., Middelburg, J.B.M., Sinninghe Damsté, J.S., 2015. Influence of deep-water derived isoprenoid tetraether lipids on the paleothermometer in the Mediterranean Sea, Geochimica et Cosmochimica Acta 150, 125-141.

Keough, B.P., Schmidt, T.M., Hicks, R.E., 2003. Archaeal nucleic acids in picoplankton from great lakes on three continents. Microbial Ecology 46, 238-248.

Loomis, S.E., Russell, J.M., Sinninghe Damsté, J.S., 2011. Distributions of br GDGTs in soils and lake sediments from western Uganda: Implications for a lacustrine paleothermometer. Organic Geochemistry 42, 739-751.

Loomis, S.E, Russell, J.M., Ladd, B., Street-Perrott, F.A., Sinninghe Damsté, J.S., 2012. Calibration and application of the br GDGT temperature proxy on East African lake sediments. Earth and Planetary Science Letters 357–358, 277-288.

Loomis, S.E., Russell, J.M., Eggermont, H., Verschuren, D., Sinninghe Damsté, J.S., 2014. Effects of temperature, pH and nutrient concentration on br GDGT distributions in East African lakes: Implications for paleoenvironmental reconstruction. Organic Geochemistry 66, 25-37.

Lopes dos Santos, R.A., Prange, M., Castañeda, I.S., Schefuß, E., Mulitza, S., Schulz, M., Niedermeyer, E.M., Sinninghe Damsté, J.S., Schouten, S., 2010. Glacial-interglacial variability in Atlantic meridional overturning circulation and thermocline adjustments in the tropical North Atlantic. Earth and Planetary Science Letters 300, 407–414.

Ménot, G., Bard, E., 2012. A precise search for drastic temperature shifts of the past 40,000 years in southeastern Europe, Paleoceanography 27, PA2210.

Meyers, P.A., 1994. Preservation of elemental and isotopic source identification of sedimentary organic matter. Chemical Geology 114, 289-302.

Moy, C.M., Dunbar, R.B., Guilderson, T.P., Waldmann, N., Mucciarone, D.A., Recasens, C., Ariztegui, D., Austin Jr., J.A., Anselmetti, F.S., 2011. A geochemical and sedimentary record of high southern latitude Holocene climate evolution from Lago Fagnano, Tierra del Fuego. Earth and Planetary Science Letters 302, 1-13.

New, M., Lister, D., Hulme, M., Makin, I., 2002. A high-resolution data set of surface climate over global land areas. Climate Research 21, 1-25.

Palma, S., Silva, N., 2004. Distribution of siphonophores, chaetognaths, euphausiids and oceanographic conditions in the fjords and channels of southern Chile. Deep-Sea Research II 51, 513-535.

Parra, O., Valdovinos, C., Urrutia, R., Cisternas, M., Habit, E., Mardones, M., 2003. Caracterización y tendencias tróficas de cinco lagos costeros de Chile Central. Limnetica 22, 51-83.

Pearson, E.J., Juggins S., Talbot, H.M., Weckström, J., Rosén, P., Ryves, D.B., Roberts, S.J., Schmidt, R., 2011. A lacustrine GDGT-temperature calibration from the Scandinavian Arctic

to Antarctic: Renewed potential for the application of GDGT paleothermometry in lakes. Geochimica et Cosmochimica Acta 75, 6225-6238.

Pérez, G., Queimaliños, C., Balseiro, E., Modenutti, B., 2007. Phytoplankton absorption spectra along the water column in deep North Patagonian Andean lakes (Argentina). Limnologica - Ecology and Management of Inland Waters 37, 3-16.

Peterse, F., Kim, J.-H., Schouten, S., Kristensen, D.K., Koç, N., Sinninghe Damsté, J.S., 2009. Constraints on the application of the MBT/CBT palaeothermometer at high latitude environments (Svalbard, Norway). Organic Geochemistry 40, 692-699.

Peterse F., Prins, M.A., Beets, C.J., Troelstra, S.R., Zheng, H., Gu, Z., Schouten, S., Sinninghe Damsté, J.S., 2011. Decoupled warming and monsoon precipitation in East Asia over the last deglaciation. Earth and Planetary Science Letters 301, 256-264.

Peterse, F., van der Meer, M.J.T., Schouten, S., Weijers, J.W.H., Fierer, N., Jackson, R.B., Kim, J.-H., Sinninghe Damsté, J.S., 2012. Revised calibration of the MBT-CBT paleotemperature proxy based on br tetraether membrane lipids in surface soils. Geochimica et Cosmochimica Acta 96, 215-229.

Pitcher, A., Hopmans, E.C., Mosier, A.C., Park, S.J., Rhee, S-.K., Francis, C.A., Schouten, S., Sinninghe Damsté, J.S., 2011a. Core and intact polar glycerol dibiphytanyl glycerol tetraether lipids of ammonia-oxidizing Archaea enriched from marine and estuarine sediments. Applied Environmental Microbiology 77, 3468-3477.

Pitcher, A., Villanueva, L., Hopmans, E.C., Schouten, S., Reichart, G.J., Sinninghe Damsté, J.S., 2011b. Niche segregation of ammonia-oxidizing archaea and anammox bacteria in the Arabian Sea oxygen minimum zone. International Society for Microbial Ecology Journal 5, 1896–1904.

Powers, L.A., Werne, J.P., Johnson, T.C., Hopmans, E.C., Sinninghe Damsté, J.S., Schouten, S., 2004. Crenarchaeotal membrane lipids in lake sediments: A new paleotemperature proxy continental paleoclimate reconstruction ?. Geology 32, 613-616.

Powers, L., Werne, J.P., Vanderwoude, A.J., Sinninghe Damsté, J.S., Hopmans, E.C., Schouten, S., 2010. Applicability and calibration of the TEX_{86} paleothermometer in lakes. Organic Geochemistry 41, 404-413.

Quiñones, R.A., Levipan, H.A., Urrutia, H., 2009. Spatial and temporal variability of planktonic archaeal abundance in the Humboldt Current System off Chile. Deep Sea Research Part II 56, 1073-1082.

Sepúlveda, J., Pantoja, S., Hughen, K.A., 2011. Sources and distribution of organic matter in northern Patagonia fjords, Chile (~44-47°S): A multi-tracer approach for carbon cycling assessment. Continental Shelf Research 31, 315-329.

Schouten, S., Hoefs, M.J.L., Koopmans, M.P., Bosch, H.-J., Sinninghe Damsté, J.S., 1998. Structural identification, occurrence and fate of archaeal ether-bound acyclic and cyclic biphytanes and corresponding diols in sediments. Organic Geochemistry 29, 1305-1319.

Schouten, S., Hopmans, E.C., Pancost, R.D., Sinninghe Damsté, J.S., 2000. Widespread occurrence of structurally diverse tetraether membrane lipids: Evidence for the ubiquitous presence of low-temperature relatives of hyperthermophiles. Proceedings of the National Academy of Sciences of the USA 97, 14421-14426.

Schouten, S., Hopmans, E.C., Schefuss, E., Sinninghe Damsté, J.S., 2002. Distributional variations in marine crenarchaeotal membrane lipids: A new tool for reconstructing ancient sea water temperatures?. Earth and Planetary Science Letters 204, 265-274.

Schouten, S., Forster, A., Panoto, F.E., Sinninghe Damsté, J.S., 2007. Towards calibration of the TEX_{86} palaeothermometer for tropical sea surface temperatures in ancient greenhouse worlds. Organic Geochemistry 38, 1537-1546.

Schouten, S., Pitcher, A., Hopmans, E.C., Villanueva, L., van Bleijswijk, J., Sinninghe Damsté, J.S., 2012. Distribution of core and intact polar glycerol dibiphytanyl glycerol tetraether lipids in the Arabian Sea Oxygen Minimum Zone: I: Selective preservation and degradation in the water column and consequences for the TEX_{86}. Geochimica et Cosmochimica Acta 98, 228-243.

Schouten S., Hopmans, E.C., Sinninghe Damsté, J.S., 2013. The organic geochemistry of glycerol dialkyl glycerol tetraether lipids: A review. Organic Geochemistry 54, 19-61.

Sievers, H.A., 2008. Temperature and salinity in the austral Chilean channels and fjords, In: Silva, N., Palma, S., (Eds.), Progress in the Oceanographic Knowledge of Chilean Interior Waters, from Puerto Montt to Cape Horn. Comité Oceanográfico Nacional - Pontificia Universidad Católica de Valparaíso, Valparaíso, Chile, 161 pp.

Silva, N., 2008. Dissolved oxygen, pH, and nutrients in the austral Chilean channels and fjords, In: Silva, N., Palma, S., (Eds.), Progress in the Oceanographic Knowledge of Chilean Interior Waters, from Puerto Montt to Cape Horn. Comité Oceanográfico Nacional - Pontificia Universidad Católica de Valparaíso, Valparaíso, Chile, 161 pp.

Sinninghe Damsté, J.S., Hopmans, E.C., Pancost, R.D., Schouten, S., Geenevasen, J.A.J., 2000. Newly discovered non-iso glycerol dialkyl glycerol tetraether lipids in sediments. Chemical Communications 17, 1683-1684

Sinninghe Damsté, J.S., Schouten, S., Hopmans, E.C., Van Duin, A.C.T., Geenevasen, J.A.J., 2002. Crenarchaeol: The characteristic core glycerol dibiphytanyl glycerol tetraether membrane lipid of cosmopolitan pelagic crenarchaeota. Journal of Lipid Research 43, 1641-1651.

Sinninghe Damsté, J.S., Ossebaar, J., Schouten, S., Verschuren, D., 2008. Altitudinal shifts in the branched tetraether lipid distribution in soil from Mt. Kilimanjaro (Tanzania): Implications for the MBT/CBT continental palaeothermometer. Organic Geochemistry 39, 1072-1076.

Sinninghe Damsté, J.S., Ossebaar, J., Abbas, B., Schouten, S., Verschuren, D., 2009. Fluxes and distribution of tetraether lipids in an equatorial African lake: Constraints on the application of the TEX_{86} palaeothermometer and BIT index in lacustrine settings. Geochimica et Cosmochimica Acta 73, 4232-4249.

Sinninghe Damsté, J.S., Rijpstra, W.I.C., Hopmans, E.C., Weijers, W.H., Foesel, B.U., Overmann, J., Dedysh, S.N., 2011. 13,16-Dimethyl octacosanedioic acid (iso-diabolic acid), a common membrane-spanning lipid of Acidobacteria subdivisions 1 and 3. Applied Environmental Microbiology 77, 4147–4154.

Sinninghe Damsté, J.S., Rijpstra, W.I., Hopmans, E.C., Foesel, B.U., Wüst, P.K., Overmann, J., Tank, M., Bryant, D.A., Dunfield, P.F., Houghton, K., Stott, M.B., 2014. Ether- and ester-bound iso-diabolic acid and other lipids in members of acidobacteria subdivision 4. Applied Environmental Microbiology 80, 5207-5218.

Spang, A., Hatzenpichler, R., Brochier-Armanet, C., Rattei, T., Tischler, P., Spieck, E., Streit, W., Stahl, D.A., Wagner, M., Schleper, C., 2010. Distinct gene set in two different lineages of ammoniaoxidizing archaea supports the phylum Thaumarchaeota. Trends in Microbiology 18, 331-340.

Strub, P.T., Mesias, J.M., Montecino, V., Ruttlant, J., Salinas, S., 1998. Coastal ocean circulation off Western South America. In: Robinson, A.R., Brink, K.H. (Eds.), The Global Coastal Ocean - Regional Studies and Syntheses. Wiley, New York, pp. 273-315.

Sun, Q., Chu, G., Liu, M., Xie, M., Li, S., Ling, Y., Wang, X., Shi, L., Jia, G., Lü, H., 2011. Distributions and temperature dependence of br glycerol dialkyl glycerol tetraethers in recent lacustrine sediments from China and Nepal. Journal of Geophysical Research 116, G01008.

Tierney, J.E., Russell, J.M., 2009. Distributions of br GDGTs in a tropical lake system: Implications for lacustrine application of the MBT/CBT paleoproxy. Organic Geochemistry 40, 1032-1036.

Tierney, J.E., Russell, J.M., Eggermont, H., Hopmans, E.C., Verschuren, D., Sinninghe Damsté, J.S., 2010a. Environmental controls on br tetraether lipid distributions in tropical East African lake sediments: a new lacustrine paleothermometer?. Geochimica et Cosmochimica Acta 74, 4902-4918.

Tierney, J.E., Mayes, M.T., Meyer, N., Johnson, C., Swarenski, P.W., Cohen, A.S., Russell, J.M., 2010b. Late-twentieth-century warming in Lake Tanganyika unprecedented since AD 500. Nature Geoscience 3, 422-425.

Tierney, J.E., Schouten, S., Pitcher, A., Hopmans, E.C., Sinninghe Damsté, J.S., 2012. Core and intact polar glycerol dialkyl glycerol tetraethers (GDGTs) in Sand Pond, Warwick, Rhode Island (USA): Insights into the origin of lacustrine GDGTs. Geochimica et Cosmochimica Acta 77, 561-581.

Tierney, J.E., Tingley, M.P., 2014. A Bayesian, spatially-varying calibration model for the TEX_{86} proxy. Geochimica et Cosmochimica Acta 127, 83-106.

Tyler, J.J., Nederbragt, A.J., Jones, V.J., Thurow, J.W., 2010. Assessing past temperature and soil pH estimates from bacterial tetraether membrane lipids: Evidence from the recent lake sediments of Lochnagar, Scotland. Journal of Geophysical Research 115, G01015.

Waldmann, N., Ariztegui, D., Anselmetti, F.S., Austin Jr., J.A., Moy, C.M., Stern, C., Recasens, C., Dunbar, R., 2010. Holocene climatic fluctuations and positioning of the Southern Hemisphere Westerlies in Tierra del Fuego (54°S), Patagonia. Journal of Quaternary Science 25, 1063-1075.

Walsh, E.M., Ingalls, A.E., Keil, R.G., 2008. Sources and transport of terrestrial organic matter in Vancouver Island fjords and the Vancouver-Washington Margin: A multiproxy approach using δ^{13}Corg, lignin phenols, and the ether lipid BIT index. Limnology and Oceanography 53, 1054-1063.

Weijers, J.W.H., Schouten, S., Hopmans, E.C., Geenevasen, J.A.J., David, O.R.P., Coleman, J.M., Pancost, R.D., Sinninghe Damsté, J.S., 2006a. Membrane lipids of mesophilic anaerobic bacteria thriving in peats have typical archaeal traits. Environmental Microbiology 8, 648-657.

Weijers, J.W.H., Schouten, S., Spaargaren, O.C., Sinninghe Damsté, J.S., 2006b. Occurrence and distribution of tetraether membrane lipids in soils: Implications for the use of the TEX_{86} proxy and the BIT index. Organic Geochemistry 37, 1680-1693.

Weijers, J.W.H., Schouten, S., van den Donker, J.C., Hopmans, E.C., Sinninghe Damsté, J.S., 2007. Environmental controls on bacterial tetraether membrane lipid distribution in soils. Geochimica et Cosmochimica Acta 71, 703-713.

Weijers, J.W.H., Panoto, E., van Bleijswijk, J., Schouten, S., Rijpstra, W.I.C., Balk, M., Stams, A.J.M., Sinninghe Damsté, J.S., 2009. Constraints on the biological source(s) of the orphan br tetraether membrane lipids. Geomicrobiology Journal 26, 402-414.

Weijers, J.W.H., Schefuß, E., Kim, J.-H., Sinninghe Damsté, J.S., Schouten, S., 2014. Constraints on the sources of br tetraether membrane lipids in distal marine sediments, Organic Geochemistry 72, 14-22.

Weischet W., 1970. Chile: Seine Länderkundliche Individualität und Struktur. Wissenschaftliche Buchgesellschaft, Darmstast, Germany.

Woltering, M., Werne, J.P., Kish, J.L., Hicks, R., Sinninghe Damsté, J.S., Schouten, S., 2012. Vertical and temporal variability in concentration and distribution of thaumarchaotal tetraether lipids in Lake Superior and the implications for the application of the TEX_{86} temperature proxy. Geochimica et Cosmochimica Acta 87, 136-153.

Wuchter, C., Schouten, S., Coolen, M.J.L., Sinninghe Damsté, J.S., 2004. Temperature-dependent variation in the distribution of tetraether membrane lipids of marine Crenarchaeota: Implications for TEX_{86} paleothermometry. Paleoceanography 19, 1-10.

Wuensch, K.L., 2014. Comparing Correlation Coefficients, Slopes, and Intercepts. Retrieved from http://core.ecu.edu/psyc/wuenschk/StatsLessons.htm.

Zell, C., Kim, J.-H., Moreira-Turcq, P., Abril, G., Hopmans, E.C., Bonnet, M.-P., Lima Sobrinho, R., Sinninghe Damsté, J.S., 2013. Disentangling the origins of br tetraether lipids and crenarchaeol in the lower Amazon River: Implications for GDGT-based proxies. Limnology and Oceanography 58, 343-353.

Zhu, C., Weijers, J.W.H., Wagner, T., Pan, J.-M., Chen, J.-F., Pancost, R.D., 2011. Sources and distributions of tetraether lipids in surface sediments across a large river-dominated continental margin. Organic Geochemistry 42, 376-386.

Zink, K.-G., Vandergoes, M.J., Mangelsdorf, K., Dieffenbacher-Krall, A.C., Schwark, L., 2010. Application of bacterial glycerol dialkyl glycerol tetraethers (GDGTs) to develop modern and past temperature estimates from New Zealand lakes. Organic Geochemistry 41, 1060-1066.

Sediment	Lat.	Long.	Core	Water depth (m)	Environment	0 m water temperature (°C)	0-200m water temperature (°C)	BIT	TEX_{86}	TEX^{H}_{86}	CBT	MBT'	MBT
1	25°59'S	70°48'W	GeoB7118-1	460	Marine	17.6	13.3	0.024	0.548	-0.261	0.006	0.324	0.315
2	25°59'S	70°50'W	GeoB7122-2	673	Marine	17.6	13.3	0.016	0.538	-0.270	-0.102	0.298	0.289
3	28°25'S	71°19'W	GeoB7129-1	476	Marine	16.4	12.6	0.023	0.534	-0.273	0.078	0.315	0.307
4	31°58'S	71°40'W	GeoB7147-1	398	Marine	15.6	12.2	0.022	0.514	-0.289	0.190	0.316	0.308
5	36°32'S	73°40'W	GeoB7162-4	798	Marine	14.4	11.5	0.017	0.478	-0.321	0.051	0.395	0.388
6	37°93'S	73°27'W	LA-SL008	15	Lanalhue lake	12.5	*n.d.*	0.950	0.438	-0.359	0.708	0.324	0.322
7	38°17'S	73°33'W	LL-SL002	38	Lleu Lleu lake	12	*n.d.*	0.917	0.458	-0.339	0.684	0.308	0.304
8	40°59'S	74°33'W	GeoB7197-1	816	Marine	13.3	10.8	0.024	0.453	-0.344	0.151	0.369	0.362
9	41°05'S	71°20'W	NH94-1	50	Nahuel Huapi lake	7.9	*n.d.*	0.477	0.391	-0.408	0.598	0.223	0.211
10	41°21'S	71°33'W	PMAS93.4	30	Mascardi lake	8.5	*n.d.*	0.475	0.416	-0.381	1.085	0.288	0.286
11	41°42'S	72°46'W	MD07-3105	329	Fjord	12.8	10.7	0.043	0.427	-0.370	0.362	0.451	0.447
12	41°42'S	72°40'W	MD07-3108	458	Fjord	12.8	10.7	0.062	0.450	-0.347	0.383	0.440	0.436
13	44°09'S	75°09'W	GeoB7182-1	301	Marine	12.1	9.9	0.056	0.472	-0.326	0.321	0.492	0.487
14	44°09'S	75°09'W	MD07-3094	1132	Marine	12.1	9.9	0.026	0.446	-0.350	0.182	0.411	0.404
15	44°17'S	75°23'W	GeoB7187-1	476	Marine	12.1	9.9	0.031	0.436	-0.361	0.146	0.396	0.389
16	44°19'S	75°22'W	GeoB7189-1	868	Marine	12.1	9.9	0.023	0.450	-0.346	0.099	0.362	0.354
17	44°19'S	75°22'W	MD07-3091	481	Marine	12.1	9.9	0.041	0.446	-0.351	0.242	0.393	0.387
18	45°23'S	73°28'W	MD07-3114	294	Fjord	11.7	9.8	0.045	0.419	-0.378	0.438	0.372	0.368
19	47°53'S	74°29'W	MD07-3122	663	Fjord	10.6	9.2	0.069	0.426	-0.371	0.426	0.426	0.426
20	47°53'S	74°29'W	MD07-3120	662	Fjord	10.6	9.2	0.070	0.421	-0.376	0.408	0.430	0.422
21	48°27'S	76°16'W	MD07-3086	1163	Marine	10.5	8.7	0.023	0.435	-0.361	0.127	0.320	0.311
22	48°57'S	71°13'W	CAR99-10P	51	Cardiel lake	8.5	*n.d.*	0.344	0.402	-0.396	0.091	0.199	0.187
23	49°10'S	76°34'W	MD07-3084	1790	Marine	10.1	8.7	0.022	0.416	-0.381	-0.148	0.281	0.270
24	50°05'S	75°06'W	MDD-1SL	65	Fjord	9.3	9.5	0.041	0.412	-0.385	0.400	0.380	0.373
25	50°19'S	75°22'W	MDD-3SL	65	Fjord	9.3	9.5	0.048	0.408	-0.389	0.170	0.399	0.393
26	50°36'S	74°59'W	Conce-1SL	191	Fjord	9.5	9.5	0.061	0.431	-0.365	0.076	0.368	0.362
27	50°49'S	74°00'W	Peel-4SL	39	Fjord	9.2	9.5	0.080	0.395	-0.403	0.584	0.304	0.301
28	52°49'S	72°54'W	CH-4	16	Chandler lake	9	*n.d.*	0.996	0.591	-0.228	1.092	0.344	0.341
29	52°53'S	73°46'W	TA-SL1	22	Tamar lake	6.4	*n.d.*	0.947	0.539	-0.269	1.233	0.273	0.271
30	53°26'S	72°55'W	LH-SL	35	Humphrey lake	4.6	*n.d.*	0.909	0.485	-0.315	1.200	0.231	0.230
31	53°34'S	70°40'W	MD07-3131	463	Fjord	7.8	7.3	0.042	0.369	-0.433	0.147	0.369	0.361
32	53°36'S	70°55'W	LHAM-SL	23	Hambre lake	5.1	*n.d.*	0.996	0.561	-0.251	1.030	0.226	0.225

33	54°32'S	67°59'W	LF06-G14	70	Fagnano lake	5.8	*n.d.*	0.824	0.343	-0.464	0.831	0.236	0.227

N°	Eq.	r^2	SEE (°C)	n	Reference
1	BIT = (VI + VII + VIII)/(cren + VI + VII + VIII)				Hopmans et al., 2004
2	TEX_{86} = (2 + 3 + cren isomer)/(1 + 2 + 3 + cren isomer)				Schouten et al., 2002
3	TEX^{H}_{86} = log ((2 + 3 + cren isomer)/(1 + 2 + 3 + cren isomer))				Kim et al., 2010
4	MBT = (VI + VIb + VIc)/(VI + VIb + VIc + VII + VIIb + VIIc + VIII + VIIIb + VIIIc)				Weijers et al., 2007a
5	CBT = -log [(VIb + VIIb)/(VI + VII)]				Weijers et al., 2007a
6	MBT' = (VI + VIb + VIc)/(VI + VIb + VIc + VII + VIIb + VIIc + VIII)				Peterse et al., 2012
7	T_{surf}^{a} = 68.4 x TEX^{H}_{86} + 38.6	0.9	2.5	255	Kim et al., 2010
8	T_{surf}^{a} = 59.6 x TEX^{H}_{86} + 33.0	0.9	0.8	23	This study
9	$T_{subsurf}^{b}$ = 54.7 x TEX^{H}_{86} + 30.7	0.8	2.2	255	Kim et al., 2012a
10	$T_{subsurf}^{b}$ = 32.1 x TEX^{H}_{86} + 21.5	0.9	0.6	23	This study
11	T = 59.6 x TEX^{H}_{86} + 32.0	0.8	2.7	78	Schouten et al., 2013
12	T_{surf}^{a} = 55.2 x TEX_{86} - 14.0	0.9	3.6	12	Powers et al., 2010
13	T_{surf}^{a} = 50.7 x TEX_{86} - 11.8	0.9	0.6	5	This study
14	T_{air}^{c} = 0.8 - 5.7 x CBT + 31.0 x MBT'	0.6	5.0	176	Peterse et al., 2012
15	T_{surf}^{a} = 6.8 - 7.1 x CBT + 37.1 x MBT	0.6	5.2	139	Sun et al., 2011
16	T_{sum}^{d} = 20.9 - 98.1 x $fr_{GDGT\text{-}VIb}$ - 12 x $fr_{GDGT\text{-}VII}$ - 20.5 x $fr_{GDGT\text{-}VIII}$	0.9	2.0	85	Pearson et al., 2011

a T_{surf} = surface water temperature
b $T_{subsurf}$ = subsurface (0-200m) water temperature
c T_{air} = surface air temperature
d T_{sum} = surface water summer temperature

Lake	Lanalhue	Lleu Lleu	Nahuel Huapi	Mascardi	Cardiel	Chandler	Tamar	Humphrey	Hambre	Fagnano
Sediment	6	7	9	10	22	28	29	30	32	33
Latitude	37°93'S	38°17'S	41°05'S	41°21'S	48°57'S	52°49'S	52°53'S	53°26'S	53°36'S	54°32'S
Longitude	73°27'W	73°33'W	71°20'W	71°33'W	71°13'W	72°54'W	73°46'W	72°55'W	70°55'W	67°59'W
Lake altitude (m.a.s.l.)	8	5	770	808	276	45	35	68	68	26
Lake surface (km^2)	32	37	646	39	370	0.02	0.07	<0.05	0.02	560
Catchment area (km^2)	360	580	2758	700	4500	0.45	0.81	n.d.	0.11	2900
Surface/catchment ratio	0.09	0.06	0.23	0.06	0.08	0.04	0.09	-----	0.18	0.19
Mean annual air temperature (°C)	12.5	12	7.9	8.5	8.5	9	6.4	4.6	5.1	6
Mean annual lake surface temperature °C)	11.5	12	7.9	8.5	n.d.	n.d.	n.d.	n.d.	n.d.	5.8
BIT	0.95	0.92	0.48	0.48	0.34	1	0.95	0.91	1	0.82
GDGT-0/cren	3.82	0.84	0.68	0.86	0.43	4.26	0.74	1.07	4642.69	0.63

Eq.	Similarity of slope: Degree of freedom	*t*-value	Probability	Similarity of intercept: Degree of freedom	*t*-value	Probability
TEX^{H}_{86} *surface* Kim et al. (2010) vs. this study	274	2.048	*0.04*	274	-	-
TEX^{H}_{86} *subsurface* Kim et al. (2010) vs. this study	274	7.144	*0.00*	274	-	-
TEX^{H}_{86} *surface* Kim et al. (2010) vs. TEX^{H}_{86} SPM Schouten et al. (2013)	329	2.218	*0.03*	329	-	-
TEX^{H}_{86} *surface* this study vs. TEX^{H}_{86} SPM Schouten et al. (2013)	97	0.000	1.00	97	2.947	*0.00*
TEX^{H}_{86} *subsurface* Kim et al. (2012a) vs. TEX^{H}_{86} SPM Schouten et al. (2013)	329	1.256	0.21	329	26.509	*0.00*
TEX^{H}_{86} *subsurface* this study vs. TEX^{H}_{86} SPM Schouten et al. (2013)	97	6.054	*0.00*	97	-	-
TEX_{86} *lake* Powers et al. (2010) vs. this study	14	0.038	0.97	14	0.252	0.81

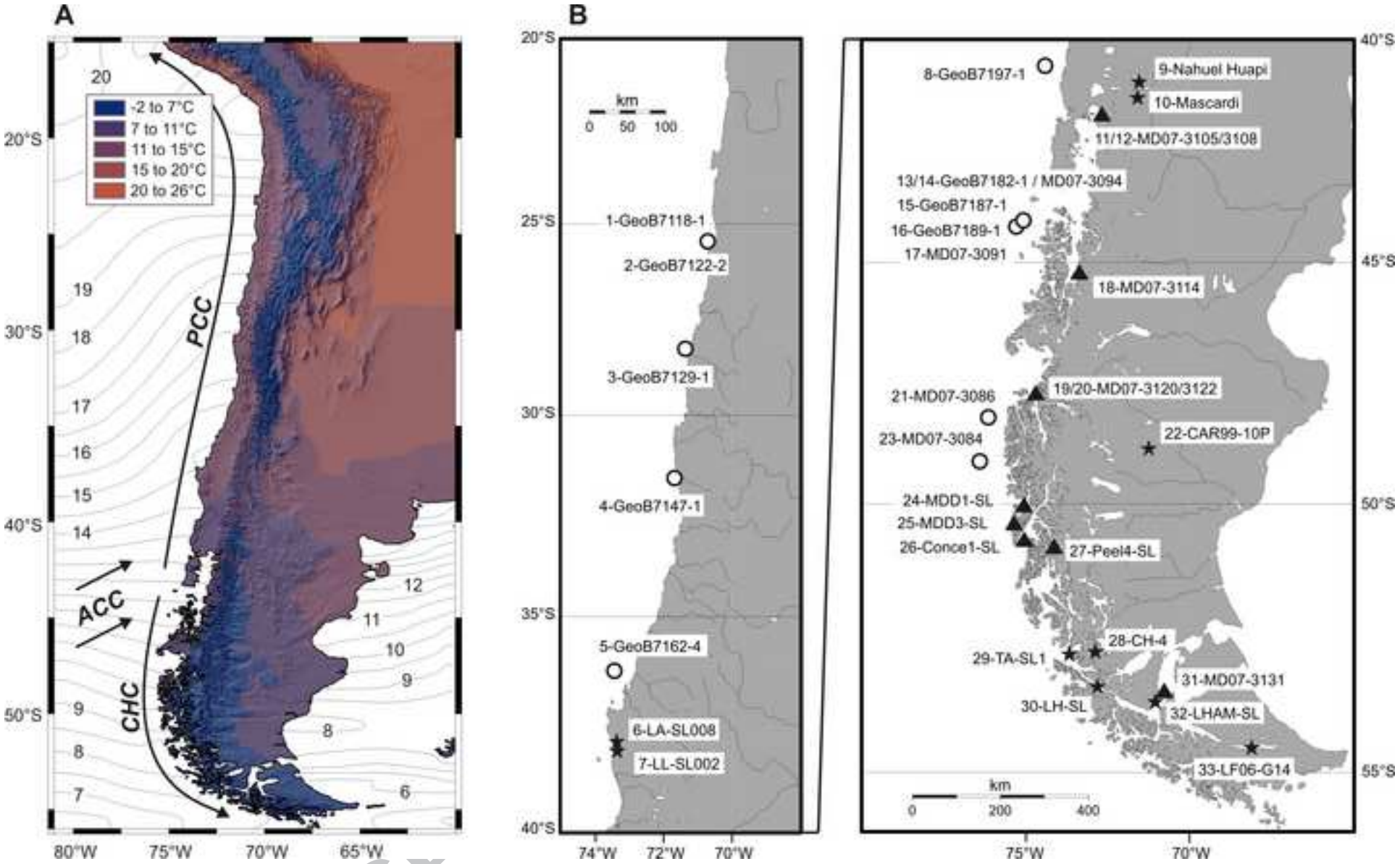

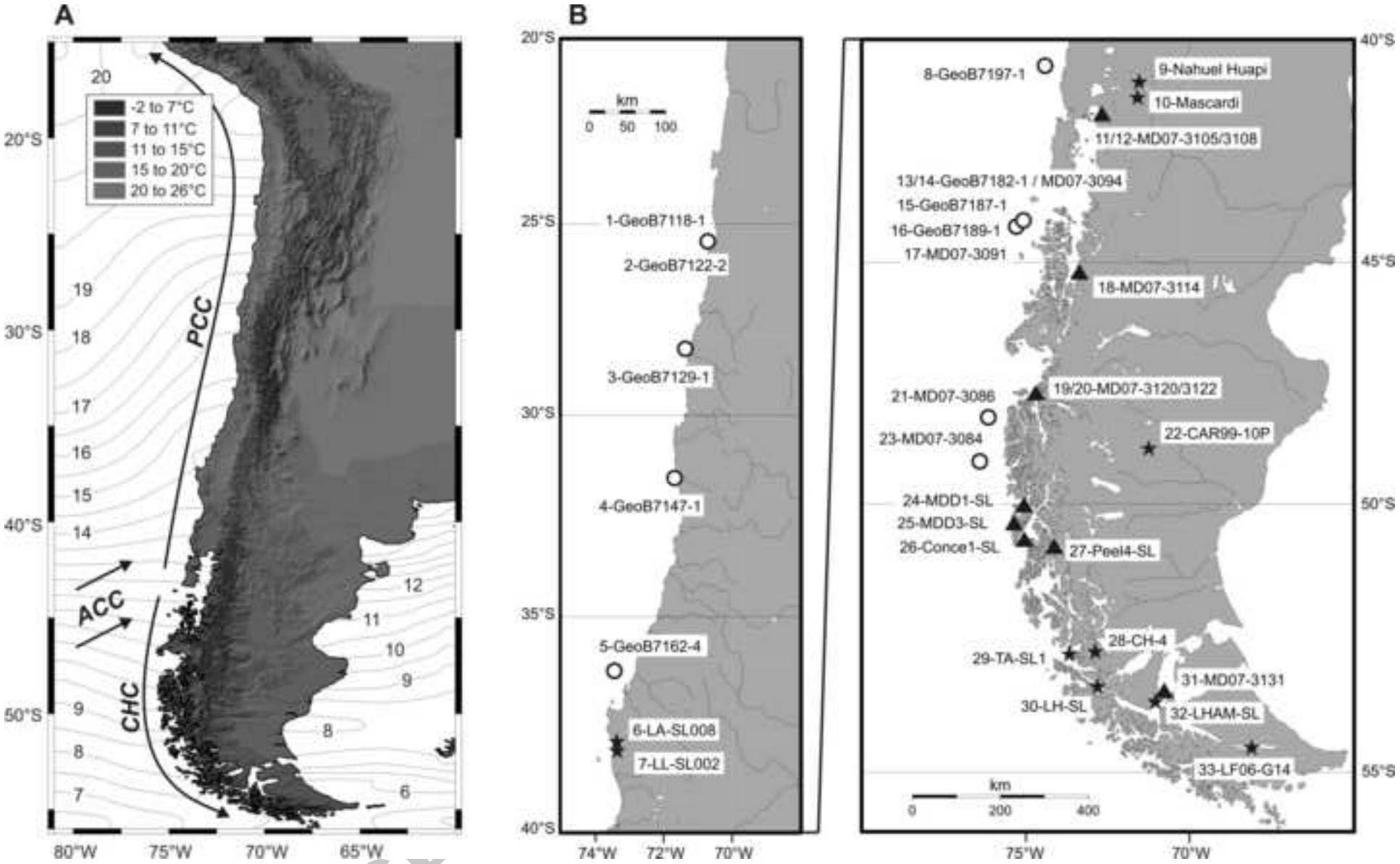

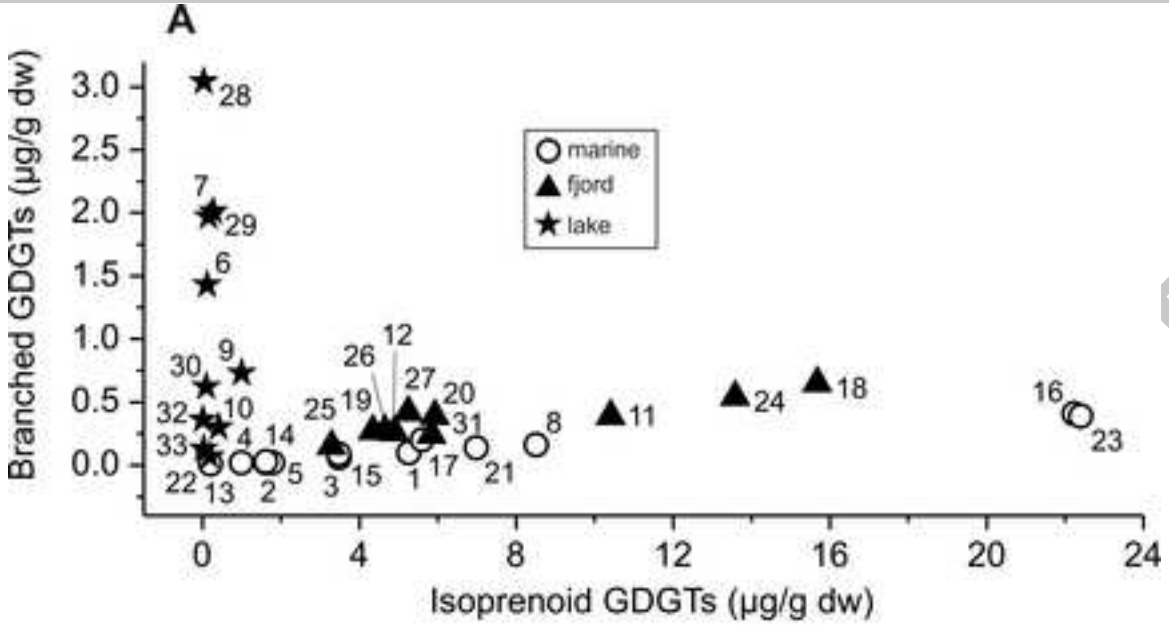

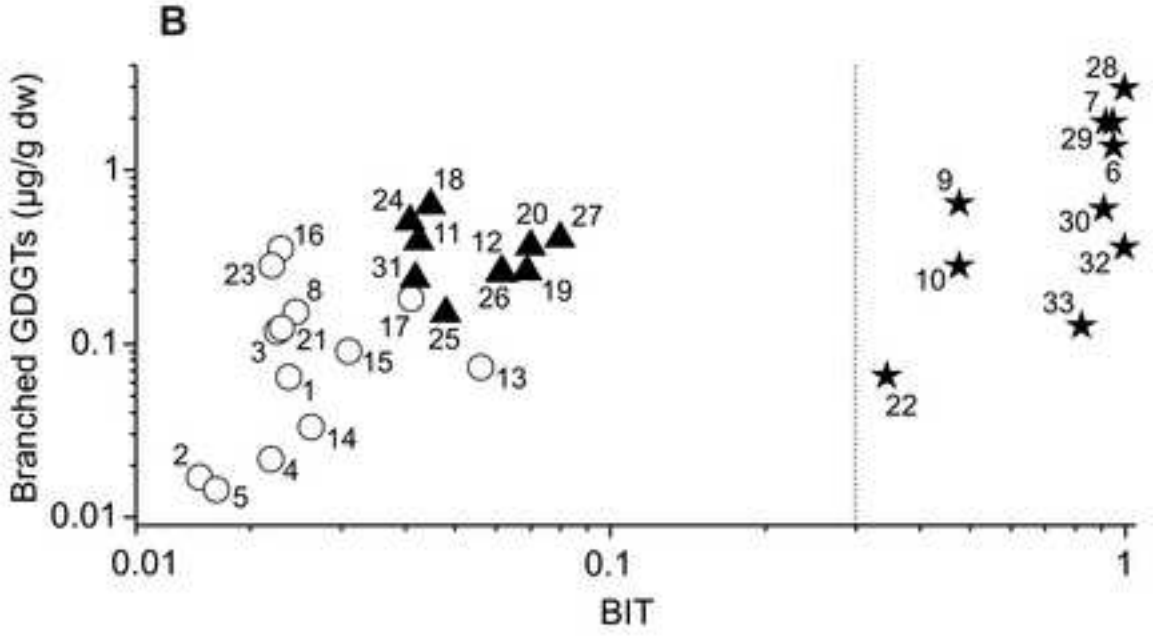

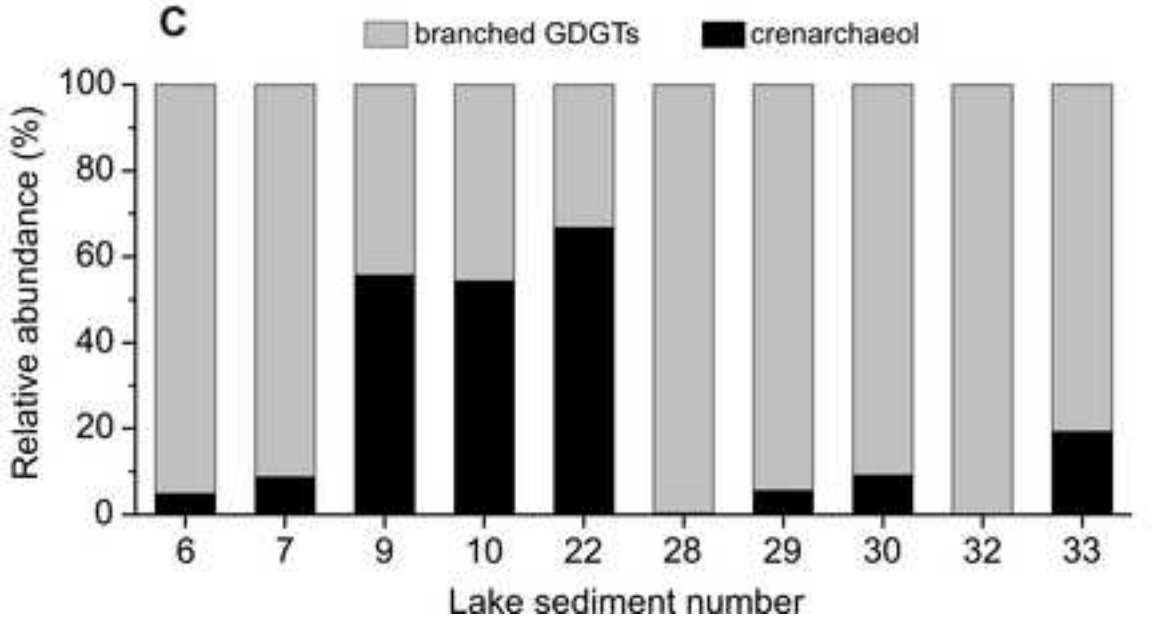

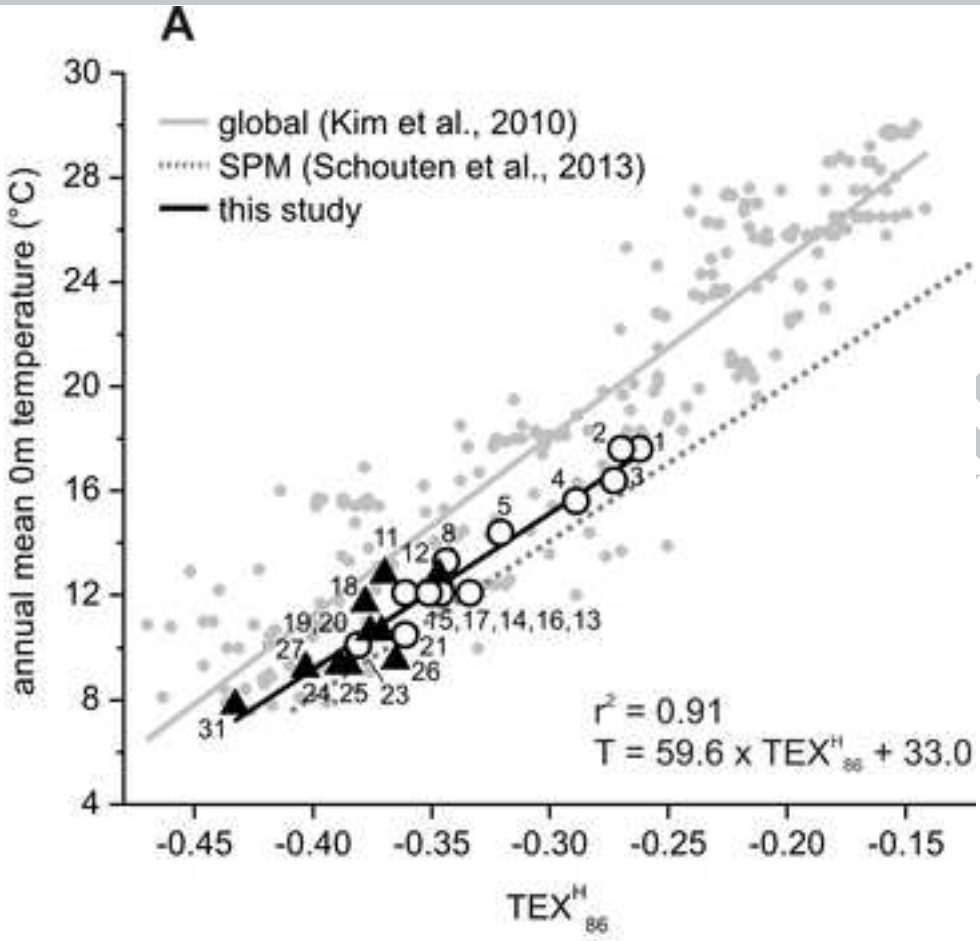

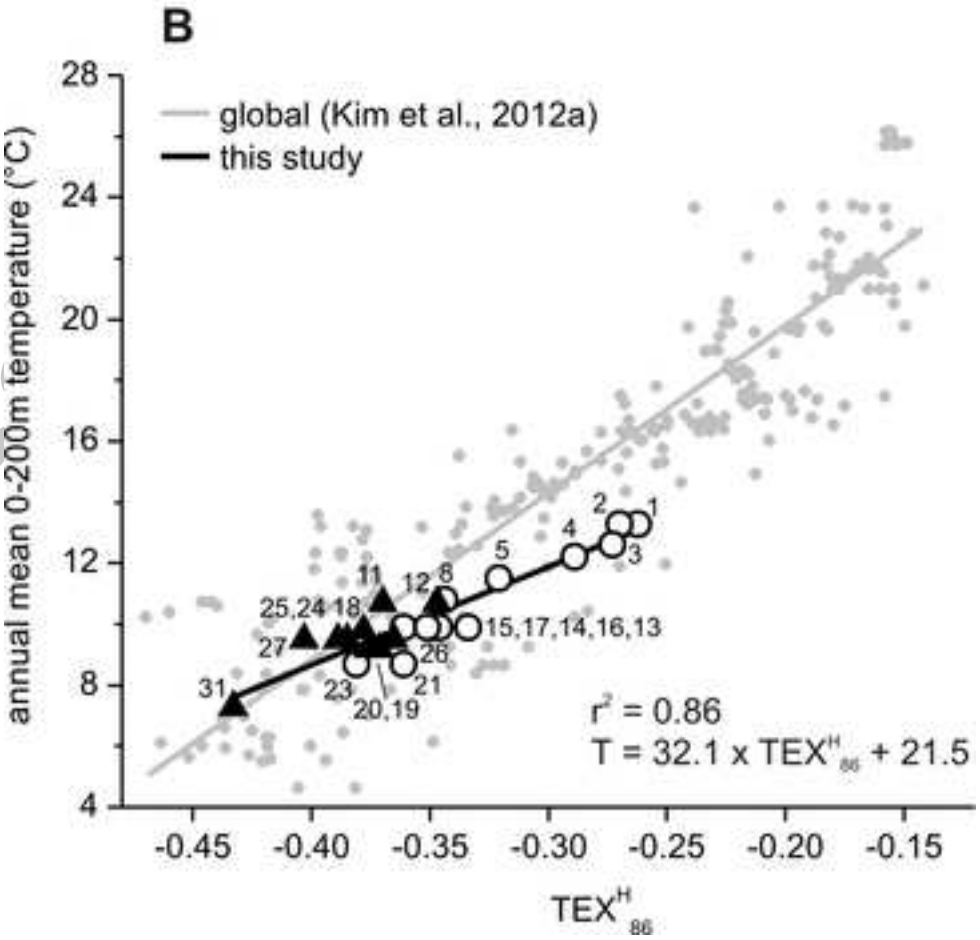

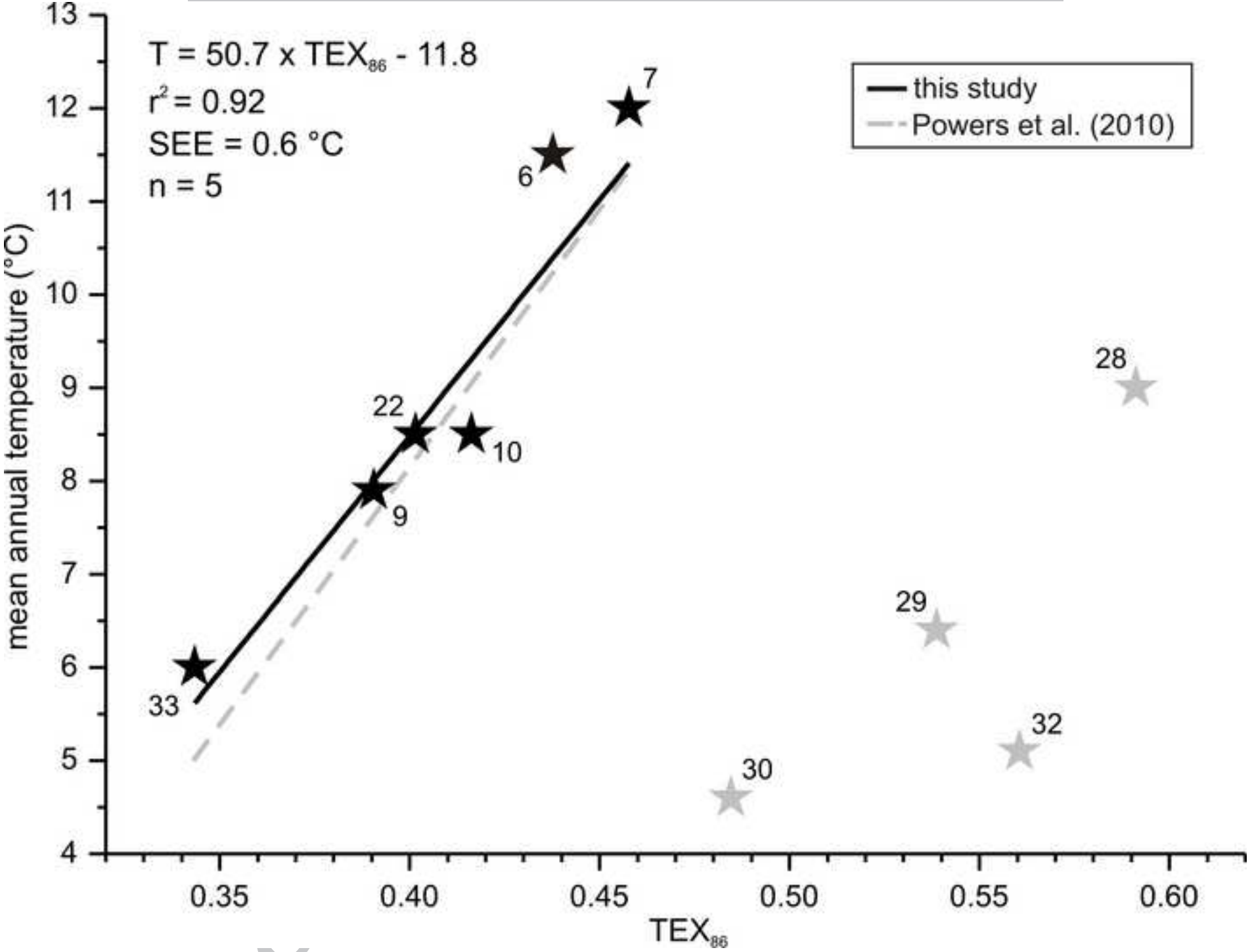

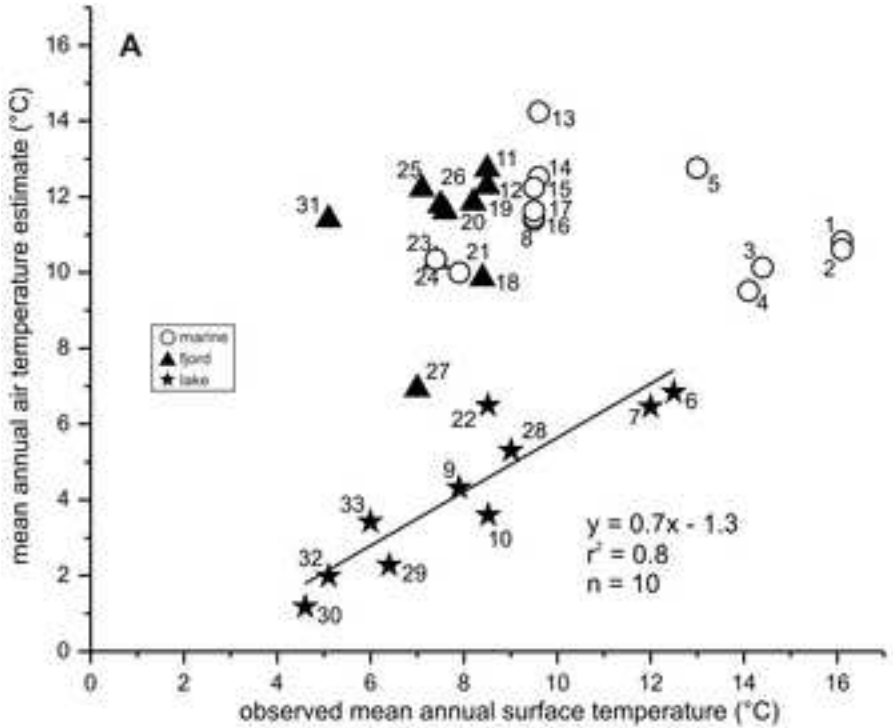

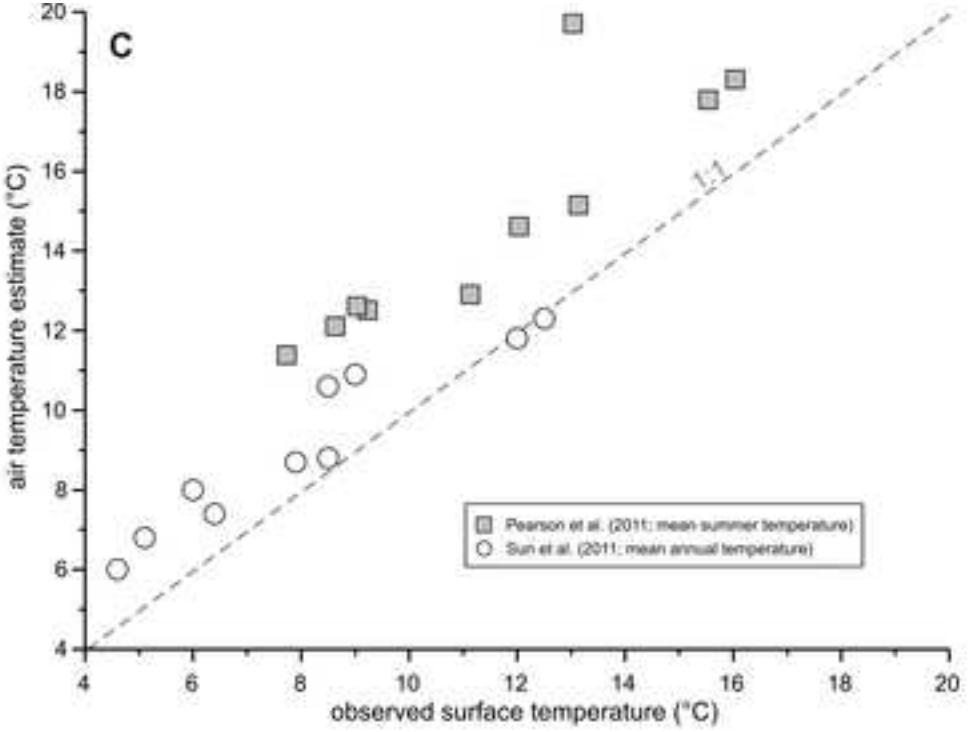

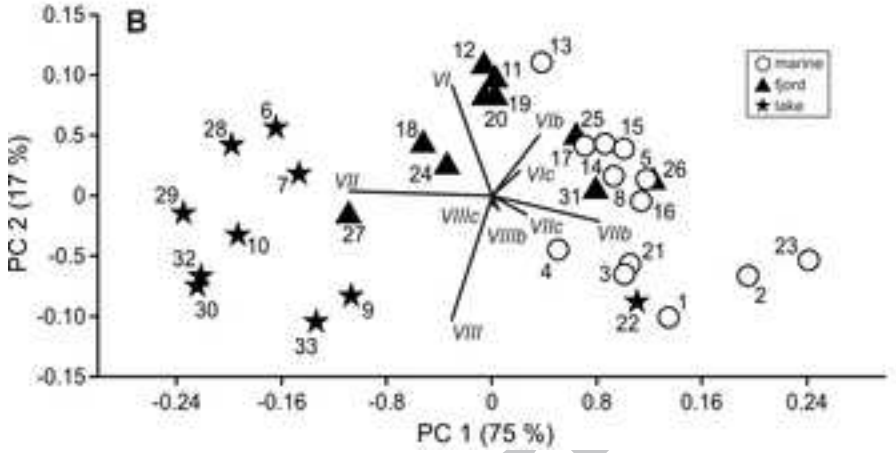

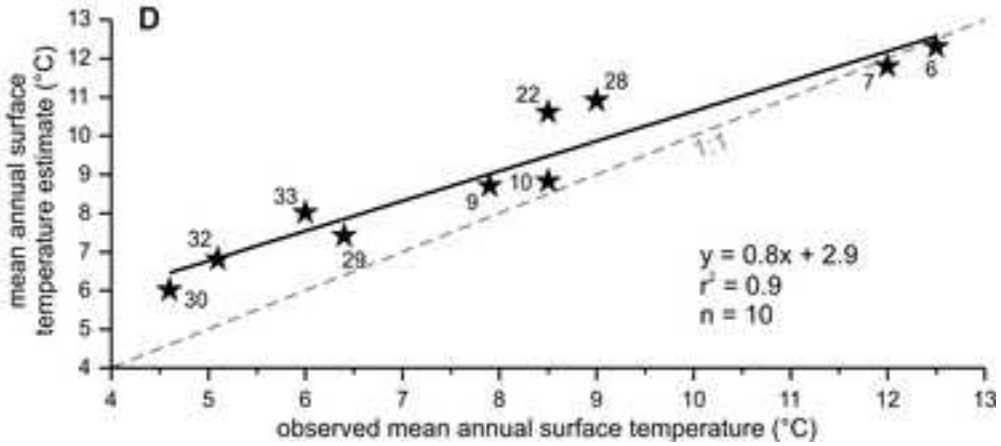

Highlights

- Analysis of surface sediments from lake, fjord and marine environments in Chile.
- Development of regional marine TEX^{H}_{86} and lake TEX_{86} calibrations.
- Potential in situ production of certain branched GDGTs.